Received: 28 August 2020 | Revised: 20 November 2020 | Accepted: 13 December 2020

DOI: 10.1002/cne.25113

RESEARCH ARTICLE

JCN RESEARCH IN SYSTEMS NEUROSCIENCE THE JOURNAL OF COMPARATIVE NEUROLOGY WILEY

Expression patterns and evolution of urocortin and corticotropin-releasing hormone genes in a cichlid fish

Brian P. Grone[1] | Julie M. Butler[2,3] | Christy R. Wayne[2] | Karen P. Maruska[2]

[1]Gladstone Institutes, San Francisco, California, USA

[2]Department of Biological Sciences, Louisiana State University, Baton Rouge, Louisiana, USA

[3]Department of Biology, Stanford University, Stanford, California, USA

Correspondence
Brian P. Grone, Gladstone Institutes, 1650 Owens St., San Francisco, CA, 94158.
Email: bpgrone@gmail.com

Funding information
Louisiana Board of Regents, Grant/Award Number: 1247192; National Science Foundation, Grant/Award Numbers: IOS-1456558, IOS-1456004

Abstract

The corticotropin-releasing hormone and urocortin family of peptides consists of five members in many vertebrates: CRH (*crha*/*crhb* in teleosts), CRH2, UCN/UTS1, UCN2, and UCN3. These genes differ in expression pattern, as well as receptor affinity, allowing them to serve a wide range of functions in a variety of species. To better understand the roles of these genes in a single species, we examined their expression patterns in the cichlid fish *Astatotilapia burtoni*. In situ hybridization to map mRNA expression patterns of *crhb*, *uts1*, *ucn2*, and *ucn3* in the brain revealed conserved and distinct spatial features of expression. *crhb*- and *uts1*-expressing cells were the most broadly distributed, with several areas of co-regionalization. *ucn3* was less abundant but was found in discrete regions throughout the extent of the brain, with high expression in the cerebellum, while *ucn2* was restricted to only a few areas. RT-PCR showed that while *crhb*, *uts1*, and *ucn3* are found in several body tissues and

Abbreviations: 4v, fourth ventricle; ac, anterior commissure; aGn, anterior glomerular nucleus; AP, area postrema; ATn, anterior tuberal nucleus; CC, cerebellar crest; CCeG, granular layer of corpus cerebellum; CCeM, molecular layer of corpus cerebellum; CCeP, purkinje layer of corpus cerebellum; CG, central gray; CM, corpus mammillare; CP, central posterior thalamic nucleus; CZ, central zone of tectum; Dc, central part of the dorsal telencephalon; Dc-1, central part of the dorsal telencephalon, subdivision 1; Dc-2, central part of the dorsal telencephalon, subdivision 2; Dc-3, central part of the dorsal telencephalon, subdivision 3; Dc-4, central part of the dorsal telencephalon, subdivision 4; Dc-5, central part of the dorsal telencephalon, subdivision 5; Dd, dorsal part of the dorsal telencephalon; Dd-d, dorsal part of the dorsal telencephalon, dorsal subdivision; Dd-v, dorsal part of the dorsal telencephalon, ventral subdivision; Dl-d, dorsal part of lateral zone of the dorsal telencephalon; Dl-g, granular zone of lateral zone of the dorsal telencephalon; Dl-v, ventral zone of lateral zone of the dorsal telencephalon; Dl-v1, ventral zone of lateral zone of the dorsal telencephalon, subdivision 1; Dl-v2, ventral zone of lateral zone of the dorsal telencephalon, subdivision 2; Dm-1, medial part of the dorsal telencephalon, subdivision 1; Dm-2r, medial part of the dorsal telencephalon, rostral subdivision 2; Dm-3, medial part of the dorsal telencephalon, subdivision 3; DON, descending octaval nucleus; DP, dorsal posterior thalamic nucleus; Dp, posterior part of the dorsal telencephalon; DT, dorsal tegmental nucleus; DWZ, deep white zone of tectum; E, entopeduncular nucleus; EG, eminentia granularis; GL, glomerular cell layer of olfactory bulb; Gn, glomerular nucleus; hc, horizontal commissure; ICL, internal cell layer of olfactory bulb; IIIn, oculomotor nucleus; IP, interpeduncular nucleus; IVn, trochlear nerve nucleus; LC, locus coeruleus nucleus; lfb, lateral forebrain bundle; LT, lateral thalamic nucleus; mlf, medial longitudinal fasciculus; MON, medial octavolateralis nucleus; NC, nucleus corticalis; NDILc, caudal part of the diffuse nucleus of the inferior lobe; NDILl, lateral part of the diffuse nucleus of the inferior lobe; NDILm, medial part of the diffuse nucleus of the inferior lobe; nGMp, magnocellular preoptic nucleus, gigantocellular division; nHd, dorsal habenular nucleus; nHv, ventral habenular nucleus; NLT, lateral tuberal nucleus; NLTd, lateral tuberal nucleus, dorsal part; NLTi, lateral tuberal nucleus, intermediate part; NLTm, lateral tuberal nucleus, medial part; NLTv, lateral tuberal nucleus, ventral part; NLVc, ventral part of nucleus of the lateral valvulae; nMLF, nucleus of medial longitudinal fasciculus; nMMp, magnocellular preoptic nucleus, magnocellular division; nPMp, magnocellular preoptic nucleus, parvocellular division; nPPa, parvocellular preoptic nucleus, anterior part; nPPp, parvocellular preoptic nucleus, posterior part; NPT, posterior tuberal nucleus; NR, nucleus ruber; NRL, nucleus of the lateral recess; NRP, nucleus of the posterior recess; NT, nucleus taenia; nTPI, nucleus of the pretectoisthmic tract; OB, olfactory bulb; oc, optic chiasm; ON, optic nerve; PAG, periaqueductal gray; pc, posterior commissure; PE, preeminential nucleus; PG, periventricular granular cell mass of caudal lobe; PGa, anterior preglomerular nucleus; PGc, commissural preglomerular nucleus; PGd, dorsal preglomerular nucleus; PGl, lateral preglomerular nucleus; PGm, medial preglomerular nucleus; PGZ, periventricular gray zone of tectum; Pit, pituitary; POA, preoptic area; PSi, superficial pretectal nucleus, intermediate division; PSP, parvocellular superficial pretectal nucleus; PTT, paratoral tegmental nucleus; PVO, paraventricular organ; Ri, inferior reticular nucleus; Rm, medial reticular nucleus; Rs, superior reticular nucleus; SGn, secondary gustatory nucleus; sgt, secondary gustatory tract; SN, suprachiasmatic nucleus; SR, superior raphe nucleus; SWGZ, superficial gray and white zone of tectum; T, tectum; TBT, tectobulbar tract; TGn, tertiary gustatory nucleus; TL, torus longitudinalis; TLa, nucleus of the torus lateralis; TPp, periventricular nucleus of the posterior tuberculum; TS, torus semicircularis; TSc, central nucleus of torus semicircularis; TSvl, ventrolateral nucleus of torus semicircularis; Vc, central part of the ventral telencephalon; VCeG, granular layer of valvular cerebellum; VCeM, molecular layer of valvular cerebellum; Vd, dorsal part of the ventral telencephalon; Vd-c, dorsal part of the ventral telencephalon, caudal subdivision; Vd-r, dorsal part of the ventral telencephalon, rostral subdivision; Vde, descending tract of the trigeminal nerve; Vi, intermediate part of the ventral telencephalon; VIIIn, octavolateralis nerve (cranial nerve VIII); VIIn, facial nerve (cranial nerve VII); VIIs, facial sensory nucleus; Vl, lateral part of the ventral telencephalon; VL, vagal lobe; Vmd, dorsal motor nucleus of trigeminal nerve; VMn, ventromedial thalamic nucleus; VOT, ventral optic tract; Vp, postcommissural part of the ventral telencephalon; Vs, supracommissural part of the ventral telencephalon; Vs-l, lateral part of the supracommissural nucleus of the ventral telencephalon; Vs-m, medial part of the supracommissural nucleus of the ventral telencephalon; Vu, cuneate nucleus of the ventral telencephalon; Vv, ventral part of the ventral telencephalon; Xm, vagal motor nucleus.

widespread throughout the brain, *ucn2* is quite restricted in the brain, and *crha* is only expressed in the eye. Bayesian phylogenetic analyses identified detailed relationships and novel orthologs in the urocortin family. We found evidence for a UCN2 gene loss in some reptiles. Our detailed description of the complete family of genes in the central nervous system of a model organism will inform future studies on the function of these genes in *A. burtoni* and provides a foundation for comparative studies with teleosts and other vertebrates.

KEYWORDS

corticotropin-releasing hormone, fishes, gene duplication, in situ hybridization, neuropeptides, phylogeny, urotensins

1 | INTRODUCTION

A corticotropin-releasing peptide was initially purified from the hypothalamus and identified based on its ability to stimulate release of corticotropin from pituitary cells (Vale et al., 1981). In addition to the releasing-hormone function, this highly conserved 41-amino-acid neuropeptide also acts as a neuromodulator in various brain regions. Thus, the name "corticotropin-releasing factor" (CRF) is used interchangeably with "corticotropin-releasing hormone" (CRH), although neither name captures the full range of actions that this neuropeptide shows (Deussing & Chen, 2018). In the past four decades, an entire family of related peptides, with corresponding receptors and interacting proteins, have been identified in vertebrates as well as invertebrate species (Cardoso et al., 2014; Endsin et al., 2017). To understand how the diverse expression patterns of multiple CRH paralogs are related to their functions, a comparative approach is necessary. By understanding the conserved and novel features of different CRH-related genes in different species, we can provide insights on how CRH genes evolved to serve adaptive roles in diverse environments and species.

Recent studies show that the CRH system in vertebrates includes a greater diversity of peptides than previously appreciated (Cardoso et al., 2016; Endsin et al., 2017). Two rounds of whole-genome duplication in vertebrates led to the presence of two CRH genes. CRH2 was originally identified in the elephant shark (Nock et al., 2011) and subsequently shown to exist in jawed vertebrates generally (Grone & Maruska, 2015b). Furthermore, the teleost-specific whole-genome duplication generated two CRH1 paralogs—*crha* and *crhb* (Grone & Maruska, 2015a). Teleost fishes constitute an extremely large and diverse group of vertebrates, and we have already identified major differences in *crha* expression in different teleosts, that is, *Astatotilapia burtoni* and zebrafish. The fact that CRH gene duplications occurred is not unexpected, given known vertebrate whole-genome duplications. It is somewhat surprising, however, that CRH2 and *crha* remained unidentified for more than three decades after the initial sequencing of CRH. Given the widespread functional importance of CRH peptides in the stress response, anxiety behavior, and other physiological processes including appetite suppression (Spina et al., 1996), cardiovascular regulation (Nazarloo et al., 2006; Vaughan et al., 1995), regulation of the inflammatory response (Jain et al., 1991), and reproduction (Florio et al., 2004; Rivier & Vale, 1984), further studies in diverse species may help reveal the selective pressures leading to such diversity over evolutionary time.

Similarly, the two rounds of vertebrate whole-genome duplication led to multiple urocortin genes in vertebrate lineages. It was proposed that a vertebrate progenitor had two peptide genes that led to the distinct lineages containing, in one group, CRH1, CRH2, and urocortin (UCN1), and in the other, urocortin 2 (UCN2) and urocortin 3 (UCN3). Two receptors have been identified for the CRF family of peptides: CRFR1 and CRFR2 (Bale & Vale, 2004). These receptors share about 70% sequence homology and likely originated from a single ancestral receptor via whole-genome duplication (Lovejoy et al., 2014). CRF is a highly potent activator of CRFR1, while UCN1 binds with similar affinity to CRHR1 and CRHR2 (Vaughan et al., 1995). UCN2 and UCN3 are potent activators of CRFR2 (Hsu & Hsueh, 2001; Reyes et al., 2001). Urotensin (UTS1) was initially identified in fishes as a potent hypotensive and corticotropin-releasing peptide (Lederis et al., 1982). UCN1 was identified in mammals (Vaughan et al., 1995) as the mammalian homolog of UTS1 and has been studied in a variety of mammalian species, while the distribution and function of UTS1 were studied in some fishes including zebrafish (Brautigam et al., 2010) and carp (Huising et al., 2007). UCN2 and UCN3 were also examined in a few fishes, including zebrafish (Brautigam et al., 2010) and medaka (Hosono et al., 2017). CRF, UCN1, and UCN3 expression in several tissues has also been reported in the amphibian *Xenopus laevis* (Boorse et al., 2005; Stenzel-Poore et al., 1992). Similarly, CRH1, CRH2, and urocortin expression was described in some birds, including chicken (Bu et al., 2019; Grommen et al., 2017; Vandenborne et al., 2005). However, a detailed description of expression patterns for all the fish urocortin genes within neural and peripheral tissues of a single species, which would be important for understanding their diverse functions, is not yet available.

Astatotilapia burtoni is a haplochromine cichlid fish from Lake Tanganyika, whose behavior and physiology are well-studied (Maruska & Fernald, 2018). *A. burtoni* males use aggressive behavioral displays in their efforts to control territories and exhibit pronounced and reversible changes in behavior, gene expression, and reproductive physiology as a

consequence of territorial dominance (Fox et al., 1997; Maruska & Fernald, 2010). Genes encoding CRH-family peptides and receptors are among those regulated by social status opportunities in *A. burtoni* (Carpenter et al., 2014). A previous study of *A. burtoni* tissues using RT-PCR revealed *crhb* mRNA expression in several neural and peripheral tissues (C. C. Chen & Fernald, 2008). Using in situ hybridization, we found *crhb* in *A. burtoni* hypothalamus and retina, while *crha* was only in the retina (Grone & Maruska, 2015a). However, detailed neuroanatomical studies of *A. burtoni crhb* expression throughout the brain are not yet reported. Similarly, the expression patterns and function of urocortins are not characterized in *A. burtoni*. In fact, UCN genes have been studied in only a few of the more than 30,000 known fish species. This lack of information on urocortin expression patterns in fishes, the largest group of vertebrates, must be overcome to understand their evolutionary relationships and functions in vertebrates generally.

The goal of this study was to identify the evolutionary relationships and expression patterns of all CRH-family genes within a single teleost fish species. Here, we use in situ hybridization to identify the distribution of *crhb*, *uts1*, *ucn2*, and *ucn3* in the brain of *A. burtoni*, and RT-PCR to reveal expression patterns of these genes and *crha* in neural and peripheral tissues. We also provide phylogenetic descriptions of the CRH family. Our results show that *crhb*, *uts1*, and *ucn3* are found in several body tissues and widespread throughout the brain, while *crha* and *ucn2* show more restricted expression patterns. Phylogenetic analysis of CRH-family peptides in *A. burtoni* confirmed that *crha* and *crhb* form a clade with *uts1*, while *ucn2* and *ucn3* are in a separate group. Broad phylogenetic analysis of UCNs among vertebrates demonstrated that UCN/UTS1, UCN2, and UCN3 each formed distinct clades, with UCN2 and UCN3 more closely related to each other than to UCN/UTS1. These results provide insights into the molecular evolution and diverse functions of the CRH gene family within a single species and more broadly across vertebrates.

2 | MATERIALS AND METHODS

2.1 | Sequence analysis

Throughout this article, we use standard gene nomenclature. For fishes, gene symbols are italicized and protein symbols are capitalized. For other vertebrates, human conventions are used: gene symbols in all capitals and italicized and protein symbols in all capitals.

To determine the phylogenetic relationships among fish urocortin gene family members, sequences for urocortin genes were identified in Genbank and Ensembl for Atlantic herring (*Clupea harengus*), bearded dragon (*Pogona vitticeps*), betta (*Betta splendens*), budgerigar (*Melopsittacus undulatus*), Burton's mouthbrooder (*Astatotilapia burtoni*), chicken (*Gallus gallus*), coelacanth (*Latimeria chalumnae*), elephant shark (*Callorhinchus milii*), golden eagle (*Aquila chrysaetos*), human (*Homo sapiens*), medaka (*Oryzias latipes*), mouse (*Mus musculus*), pig (*Sus scrofa*), platypus (*Ornithorhynchus anatinus*), spotted gar (*Lepisosteus oculatus*), Tasmanian devil (*Sarcophilus harrisii*), and western clawed frog (*Xenopus tropicalis*). These species were chosen for their high-quality genomic databases in order to represent broad vertebrate coverage while limiting the potential for errors.

In Table 1, Ensembl identification numbers or GenBank accession numbers are listed.

mrBayes 3.2.7a (Ronquist et al., 2012) was used to infer phylogenetic relationships, and was accessed via the CIPRES web portal (Miller et al., 2010). In MrBayes, default settings were used except for the following specified parameters: rates(among-site variation) = gamma, aamodelpr(amino acid rate matrix) = mixed; nruns(number of runs) = 2; ngen(number of generations) = 1,000,000; samplefreq = 500; nchain (number of chains) = 8; temp(chain heating temperature) = 0.1; burninfrac(fraction of initial generations discarded) = 0.25. Diagnostics of the MCMC sampling were carried out using Tracer v1.7.1 (Rambaut et al., 2018). The effective sample size (ESS) for each parameter was >900 for each run, allowing adequate sampling of the Markov chain. The tree generated using MrBayes was visualized using FigTree v1.4.3 (http://tree.bio.ed.ac.uk/software/figtree/).

2.2 | Animals and tissue collection

Laboratory-bred African cichlid fish *Astatotilapia burtoni* (Günther 1894) were maintained in mixed-sex groups in flow-through 30L aquaria under conditions similar to their native Lake Tanganyika (pH 8.0, 28–30 C, 300–500 μS cm^{-1}, 12L:12D light cycle, constant aeration). Fish were fed cichlid flakes daily (Aquadine, Healdsburg, CA) and supplemented with brine shrimp several times a week. All experiments were performed in accordance with the recommendations and guidelines provided by the National Institutes of Health Guide for the Care and Use of Laboratory Animals, 2011. The protocol was approved by the Institutional Animal Care and Use Committee (IACUC protocol #18-101) at Louisiana State University, Baton Rouge, LA.

Fish were quickly netted from aquaria and measured for standard length (SL) and body mass (BM), immobilized in ice-cold water, and sacrificed by rapid cervical transection. Gonads were removed and weighed to calculate gonadosomatic index [GSI = (gonad mass/BM) × 100]. For RT-PCR, brains were removed from the cranium, macrodissected, and frozen at −80 C until RNA isolation. For in situ hybridization, brains were exposed and heads were fixed in 4% paraformaldehyde (PFA) made in 1x phosphate-buffered saline (PBS) at 4 C overnight, rinsed in 1x PBS, and cryoprotected in 30% sucrose prepared in 1x PBS for 1–2 days at 4 C. Brains were then dissected from the head and mounted in OCT media, sectioned in the transverse plane at 20 μm with a cryostat, and collected onto two to three alternate sets of charged slides (VWR Superfrost plus). Slides were dried flat at room temperature for 2 days and stored at −80 C until staining.

2.3 | Expression of *crh*-family transcripts in nervous and peripheral tissues

To determine which central and peripheral tissues express different *crh*-family transcripts, we used macrodissections, RT-PCR, and gel

TABLE 1 Sources for UCN/UTS1, UCN2, and UCN3 sequences used for analyses

Common name	Species	UCN/UTS1	UCN2	UCN3
Atlantic Herring	*Clupea harengus*	XP_012674743.1	XP_012696518.1	XP_012679926.1
Bearded Dragon	*Pogona vitticeps*	XP_020663969.1		XP_020633946.1
Budgerigar	*Melopsittacus undulatus*	ENSMUNP00000013993	XP_030901895.1	ENSMUNP00000002797
Burton's mouthbrooder	*Astatotilapia burtoni*	XP_005949439.1	ENSHBUP00000009556	ENSHBUP00000007453
Crocodile	*Crocodylus porosus*	XP_019393758.1	ENSCPRT00005030637.1	XP_019399569.1
Chicken	*Gallus gallus*	AGC65587.1	XP_015140488.2	APU52336.1
Coelacanth	*Latimeria chalumnae*	ENSLACP00000011213	JH126690.1:1523227–1522793	XP_005997394
Elephant Shark	*Callorhinchus milii*	XP_007902667.1	XP_007889030.1	XP_007888748
Golden Eagle	*Aquila chrysaetos chrysaetos*	XP_029893028.1	XP_029852200.1	XP_029871265.1
Human	*Homo sapiens*	NP_003344.1	NP_149976.1	NP_444277.2
Medaka	*Oryzias latipes*	NP_001295911.1	NP_001121991.1	NP_001121992.1
Mouse	*Mus musculus*	NP_067265	NP_659543	NP_112540
Pig	*Sus scrofa*	ENSSSCP00000032698	ENSSSCP00000045074	ENSSSCP00000020262
Platypus	*Ornithorhynchus anatinus*	XP_028928378.1	Ultra32 775736	XP_007655165.1
Spotted Gar	*Lepisosteus oculatus*	LG1:17173244:17177361:1	LG5_51350408	XP_015207759.1
Tasmanian Devil	*Sarcophilus harrisii*	XP_003767139.1	XP_023353749.1	XP_003772475.1

Note: Multiple sequence alignments were carried out on full-length predicted prepropeptide amino acid sequences using MAFFT v7.017 (Katoh & Standley, 2013) in Geneious software version 5.1.7 (Kearse et al., 2012), with the following settings: Algorithm = E-INS-i; scoring matrix = BLOSUM62; gap-open penalty = 1.53.

electrophoresis. For brain regions, we removed brains from an adult dominant male. Brains were carefully dissected from the head. The pituitary and olfactory bulbs were removed and collected. Next, the telencephalon was separated just rostral to the optic nerves using a surgical blade to carefully ensure that the preoptic area remained with the hypothalamus. The spinal cord was severed just proximal to the medulla, and the corpus cerebellum was separated at the most ventral portion where it reaches the hindbrain. Finally, the hypothalamus was separated just below the midbrain, and the hindbrain portion was separated just caudal to the tectum. Thalamic nuclei are included in the midbrain portion, but it is possible that the hypothalamus portion also includes some thalamic nuclei. Eye tissue contained whole eyes with lens removed, and the urohypophysis was collected from the caudal end of the spinal cord near the tail. Skin, heart, liver, kidney, spleen, ovary (from a female), and testis were also collected to examine peripheral tissue expression. All samples were immediately frozen and stored at −80 C until RNA isolation.

Macrodissected brain and peripheral tissues were homogenized, RNA was isolated using RNeasy Plus Micro or Mini kits (Qiagen; Germantown, MD) following manufacturer's protocols, and RNA was reverse transcribed to cDNA using qScript (Quantabio). cDNA, Platinum PCR SuperMix (ThermoFisher), nuclease-free water, and gene-specific primers (Table 2) were combined for PCR (95 C for 1 min; 35–40 cycles of 95 C for 30 s, 55 C for 30 s, 72 C for 1 min; 72 C for 1 min). We tested multiple primer sets for each gene, which showed similar tissue distributions. Only representative gels from the best primer sets are shown. About 5 μl of PCR product and 1 μl of loading dye were loaded into each well and run on a 2% agarose gel with GelRed at 65 V for 45–60 min. The products were visualized on a Biorad ChemiDoc Imaging system and verified to be the appropriate size in relation to the ladder (100 bp TrackIT). In addition, all samples were run with *β-actin* as a positive control. Negative controls (no RT enzyme in RT-PCR and no cDNA template in PCR) showed no bands in any reactions. PCR products (whole brain cDNA with gene-specific primers) were sequenced (Eurofin Genomics; Louisville, KY) for verification of primer specificity and amplification of each correct target gene.

2.4 | Chromogenic in situ hybridization to localize *crh*-family transcripts in the brain

We performed ISH on a total of eight males (SL = 50 ± 2.3 mm, BM = 2.88 ± 0.55 g) and seven females (SL = 39 ± 1.6 mm, BM = 3.96 ± 1.62 g) of mixed reproductive states. A total of five to seven animals were stained and examined for each gene (*crhb*, *uts1*, *ucn2*, and *ucn3*). ISH was done as previously described (Butler & Maruska, 2016; Grone & Maruska, 2015a; Porter et al., 2017). Digoxigenin (DIG)-labeled riboprobes were made from whole brain cDNA with gene-specific primers and purified (Table 2). Sense control probes for each gene were generated in the same manner but had the T3 RNA polymerase promoter sequence (aattaaccctcactaaaggg) added to the forward (sense) primer. Slides of cryosectioned brains were brought to room temperature and tissue was surrounded with a hydrophobic barrier (Immedge pen, Vector Laboratories). Slides were treated with

TABLE 2 Primer sequences used for RT-PCR and to generate templates for riboprobe synthesis used for in situ hybridization

Gene	Forward (5′→ 3′)	Reverse (5′→ 3′)	Product size (bp)
RT-PCR primers			
crha	TCATGGATACCCTCGGAAA	GCCAACATTTCAGGACGA	76
crhb	GACTCGAACTCTTTCCCATC	ATGAAGAACGGCATATCTCTAC	545
uts1	GCCCAACTCGCTTGTATATC	TAGTGCTCCCGCTCAAA	118
ucn2	CGTGCGTGCTTCTGTTTGGC	CTATTCGTGCCATCAGCTCTGC	345
ucn3	GCTGTCGTCCCTAAAGACCCTG	CCTTTGTTGCTGTTGCGGA	338
β-actin	AAGATGAAATCGCCGCACT	GGGTACTTCAGGGTCAGGATA	205
ISH primers[a]			
crhb	GACTCGAACTCTTTCCCATC	ATGAAGAACGGCATATCTCTAC	545
uts1	CCAGAAATCCCACACCTATTG	ACCTCGTCGAGCACTTT	800
ucn2	CGTGCGTGCTTCTGTTTGGC	CTATTCGTGCCATCAGCTCTGC	345
ucn3	GCTGTCGTCCCTAAAGACCCTG	CCTTTGTTGCTGTTGCGGA	338

[a]T3 transcription initiation sequence (aattaaccctcactaaaggg) was added to the reverse primer (for antisense) or forward primer (for sense control) for riboprobes.

the following solutions: 1x PBS (3 × 5 min), 4% PFA (20 min), 1x PBS (2 × 5 min), proteinase K (10 min), 1x PBS (10 min), 4% PFA (15 min), 1x PBS (2 × 5 min), milliQ water (3 min), 0.1 M triethanolamine-HCl pH 8.0 with acetic anhydride (10 min), 1x PBS (5 min). Tissue was then prehybridized for 3 h in a sealed chamber at 60–65 C, followed by incubation with probe solution. Slides with DIG-labeled probe were covered with hybrislips and hybridized overnight (18 h) in a 60–65 C oven. After hybridization, stringency washes were performed at 60 C as follows: 2x saline sodium citrate (SSC): 50% formamide (2 × 30 min), 1:1 mixture of 2x SSC: maleate buffer with tween (MABT; 2 × 15 min), and MABT (2 × 10 min). Slides were transferred to room temperature and washed with MABT (2 × 10 min), followed by blocking of nonspecific binding with MABT containing 2% bovine serum albumin (BSA) for 3 hrs at room temperature. After blocking, slides were incubated with anti-DIG AP antibody (Roche; diluted 1:5000 in blocking solution) overnight at 4 C in a sealed humidified chamber. Slides were then washed in MABT (3 × 30 min), treated with alkaline phosphatase (AP) buffer (2 × 5 min), and developed in NBT/BCIP solution at 37 C for 5 h. Following development, slides were treated with 1x PBS (3 × 5 min), 4% PFA (10 min), and 1x PBS (3 × 5 min). Slides were coverslipped with aqueous mounting media (Aquamount, Lerner Laboratories), dried flat overnight, and then edges sealed with clear nail polish.

2.4.1 | Imaging and analysis

To map the distribution of *crhb*, *uts1*, *ucn2*, *and ucn3*-expressing cells, slides of stained tissue were visualized on a Nikon Eclipse Ni microscope controlled by Nikon Elements software (RRID:SCR_014329), and photographs were taken with a color digital camera (Nikon DS-Fi2). Localization results are based on consensus staining from all animals (mixed sex and reproductive states). Images were adjusted for contrast, brightness, and levels as needed in Photoshop (Adobe Systems, San Jose, CA; RRID: SCR_014199). Distracting artifacts were also removed with the Photoshop clone tool. To facilitate identification of neuroanatomical structures and brain nuclei, we used a cresyl-violet stained *A. burtoni* reference brain and annotated atlas, as well as other brain atlases from this and other teleost species (Burmeister, Munshi, & Fernald, 2009; Fernald & Shelton, 1985; K. P. Maruska, Butler, Field, & Porter, 2017; Munoz-Cueto, Sarasquete, Zohar, & Kah, 2001; M.F. Wullimann, Rupp, & Reichert, 1996).

3 | RESULTS

3.1 | Phylogenetic analyses

We identified five CRH/UCN gene family members in *A. burtoni* and obtained their sequences from genomic and transcriptomic databases. Tunicate (*Ciona intestinalis*) diuretic hormone-like peptide (DHLP) was chosen as an outgroup because tunicates are closely related to vertebrates but appear to possess only one CRH-family peptide, similar to an unduplicated CRH-like peptide in a vertebrate ancestor (Lovejoy & Barsyte-Lovejoy, 2010). A phylogenetic analysis (Figure 1) confirmed the expected relationship of *A. burtoni* CRH-family peptides: *crha* and *crhb* are closely related and form a clade with *uts1*, while *ucn2* and *ucn3* are in a separate group.

To better understand the relationships among vertebrate urocortin family members, we created a phylogenetic tree including UCN/UTS1, UCN2, and UCN3 sequences from a range of fishes, birds, reptiles, and mammals (Figure 2). CRH1/CRH2 and *crha*/*crhb* sequences were not included in this tree and have been compared elsewhere (Cardoso et al., 2016; Grone & Maruska, 2015a, 2015b). This tree was based on Bayesian analysis of the full-length predicted prepropeptide sequences and included all the known urocortin genes for each species in the tree. In this tree, UCN/UTS1, UCN2, and UCN3 sequences each formed distinct clades. UCN2 and UCN3 sequences also formed a clade, more closely related to each other than to UCN/UTS1.

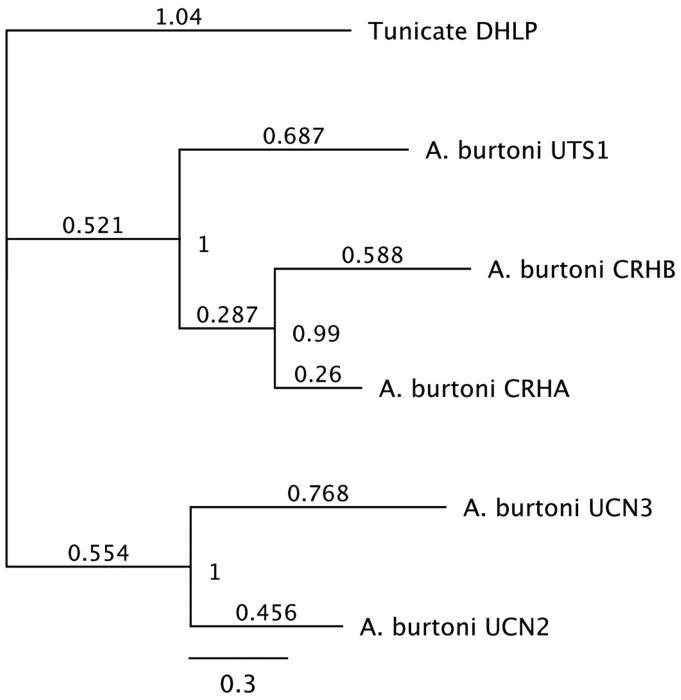

FIGURE 1 Phylogenetic tree showing relationships of all fivemembers of the *A. burtoni* CRH/UCN family. Full-length prepropeptide amino acid sequences were aligned using MAFFT and the tree was generated using MrBayes. Tunicate (*Ciona intestinalis*) diuretic hormone-like peptide (DHLP) was used as an outgroup. Node labels show posterior probabilities. Branch labels show number of substitutions per site and the scale bar indicates length of 0.3 substitutions/site

Alignments of UCN, UCN2, and UCN3 peptide sequences revealed different degrees of sequence conservation (Figure 3). In the UCN3 clade, there were relatively few amino acid differences. The short branch lengths in the phylogenetic tree reflect high conservation of this peptide among many vertebrates. In contrast, UCN2 branch lengths were quite long, with notable sequence divergence between mammalian sequences and other species. Compared to *A. burtoni* UCN2 sequence used as a reference, mammalian and other vertebrate UCN2 peptides showed high sequence diversity, with many nonidentical amino acid residues across species. UCN/UTS1 also had a relatively high level of sequence divergence. Fish UCN2 sequences formed a clade, as did mammalian UCN2 sequences, but our analysis did not resolve all the UCN2 sequences in a single clade, likely because of the extent of sequence diversity. In contrast, all UCN3 sequences were resolved as a single clade.

In reptile species, we identified novel genes in this family and discovered potential gene losses in some groups (Figure 2). We found UCN, UCN2, and UCN3 genes in saltwater crocodile (*Crocodylus porosus*), where they had not been previously reported. In contrast, snakes and lizards, including the bearded dragon (*Pogona vitticeps*), have genes in the UCN and UCN3 clades but no identifiable UCN2 genes (Figure 3).

3.2 | Expression of *crh*-family transcripts in nervous and peripheral tissues

We used RT-PCR and gel electrophoresis to localize transcripts of *crha*, *crhb*, *uts1*, *ucn2*, and *ucn3* in peripheral (Figure 4) and macrodissected nervous tissues (Figure 5). There was no *crha* expression detected in any peripheral tissue, and *crhb* was expressed in skin, spleen, ovary, and testis. *uts1* was found in ovary and testes, *ucn2* was detected in heart, spleen, and ovary and testis, and *ucn3* was found in skin, kidney, spleen, ovary and testis. In nervous tissues, *crha* was detected in the eye, and a weak band was present in the whole brain, but macrodissected brain regions showed undetectable expression (Figure 5). Strong bands showing amplification of *crhb* were detected in the eye, whole brain, telencephalon, hypothalamus, midbrain, and urohypophysis. Weaker expression for *crhb* was also seen in the olfactory bulbs, cerebellum, hindbrain, and spinal cord, while the pituitary showed a very faint band. Relatively high expression of *uts1* was found in the eye, whole brain, telencephalon, midbrain/thalamus, and hypothalamus. Weaker *uts1* bands were also evident in the cerebellum, hindbrain, spinal cord, and urohypophysis, and no expression detected in the olfactory bulbs and pituitary. For *ucn2*, strongest expression was present in the eye, whole brain, and spinal cord, moderate expression in the midbrain, hypothalamus, cerebellum, and urohypophysis, weak expression in the olfactory bulbs, telencephalon, and hindbrain, and undetectable expression in the pituitary. Strong bands for *ucn3* were detected in the whole brain, eye, midbrain/thalamus, and cerebellum, and weaker expression was present in all other tested nervous tissues (Figure 5).

3.3 | Localization of *crhb*, *uts1*, *ucn2*, and *ucn3* in the brain

We used chromogenic in situ hybridization to map the distribution of *crhb*-, *uts1*-, *ucn2*-, and *ucn3*-expressing cells throughout the *A. burtoni* brain. Sense control probes for each gene showed no staining in the brain when applied to adjacent sections labeled with anti-sense DIG-labeled probes (Figure 6). Localization patterns for all four genes are summarized in Figure 7 and described in detail below.

3.4 | Localization of *crhb* expression

3.4.1 | Olfactory bulbs and telencephalon

Scattered *crhb*-expressing cells lie in the glomerular layer of the olfactory bulbs (Figures 7(a2) and 8(a)). In the telencephalon, a dense population of darkly stained *crhb* cells lie the medial and lateral parts of the ventral telencephalon (Vc, Vl) (Figures 7(b2) and 8(b)). Staining is denser along the lateral edge of the Vl and extends dorsally toward the central part of the dorsal telencephalon (Dc) more caudally. A few *crhb*-stained cells are scattered in the dorsal and ventral parts of the ventral telencephalon area (Vd, Vv) (Figure 7(b2)).

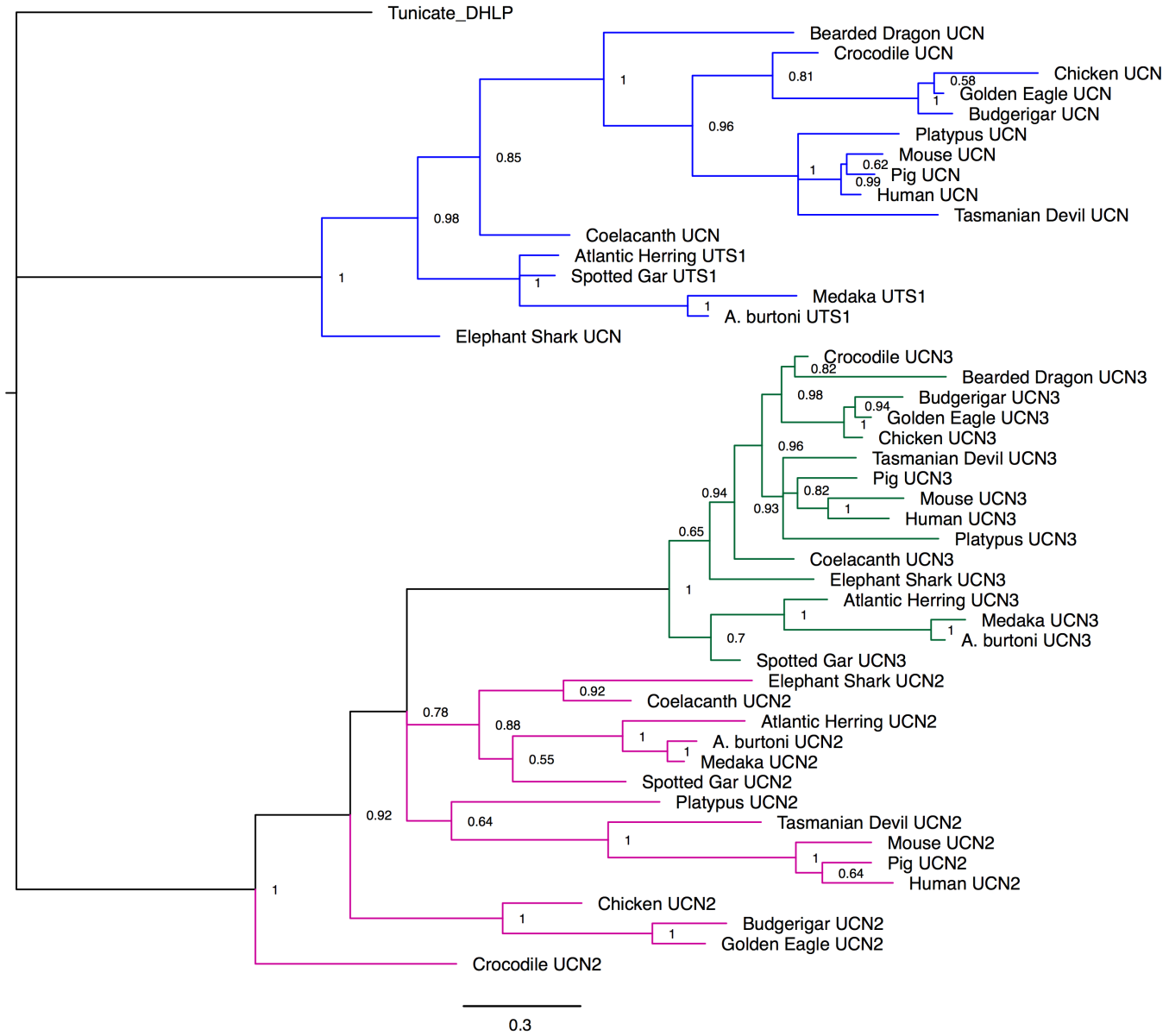

FIGURE 2 Phylogenetic tree of vertebrate urocortin prepropeptide sequences. Phylogenetic tree showing relationships of UTS1/UCN, UCN2, and UCN3 from a broad range of vertebrates including fishes, reptiles, birds, and mammals. The evolutionary history was inferred from mrBayes. Node labels show the posterior probability of each clade. The tree is drawn with branch lengths proportional to the evolutionary distances, which are in units of the number of substitutions per site. The scale bar indicates length of 0.3 substitutions/site [Color figure can be viewed at wileyonlinelibrary.com]

3.4.2 | Diencephalon

Cells expressing *crhb* are found throughout the preoptic area (POA) (Figures 7(c2–f2) and 8(c)). A group of small cells is found in the dorsal parvocellular preoptic nucleus, anterior part (nPPa) (Figure 7(c2–d2)) and scattered cells lie in the posterior part (nPPp) (Figure 7(e2–f2)). More caudally, larger *crhb*-positive cells are found in the magnocellular and parvocellular divisions of the magnocellular preoptic nucleus (nMMp, nPMp) (Figure 7(e2)). A few large, possibly gigantocellular cells, are located in the magnocellular preoptic nucleus, gigantocellular division (nGMp). A line of darkly stained *crhb* cells are located along the ventral edge of the POA in the area of the suprachiasmatic nucleus (SN) (Figure 8(c)).

Cells expressing *crhb* are also found throughout the lateral tuberal nucleus (NLT), particularly in the intermediate, medial, and ventral parts (NLTi, NLTm, NLTv) (Figures 7(f2-i2) and 8(d)). A small cluster of cells is located in the dorsal NLT part (NLTd) and dorsal part of the anterior tuberal nucleus (ATn) (Figure 7(g2)). A group of *crhb*-expressing cells also populate the area near corpus mammillare (CM) and posterior tuberal nucleus (NPT) (Figure 7(i2)). Scattered *crhb*-expressing cells are found in the nucleus corticalis (NC) and throughout other thalamic regions (Figure 7(f2–h2)). Cells containing

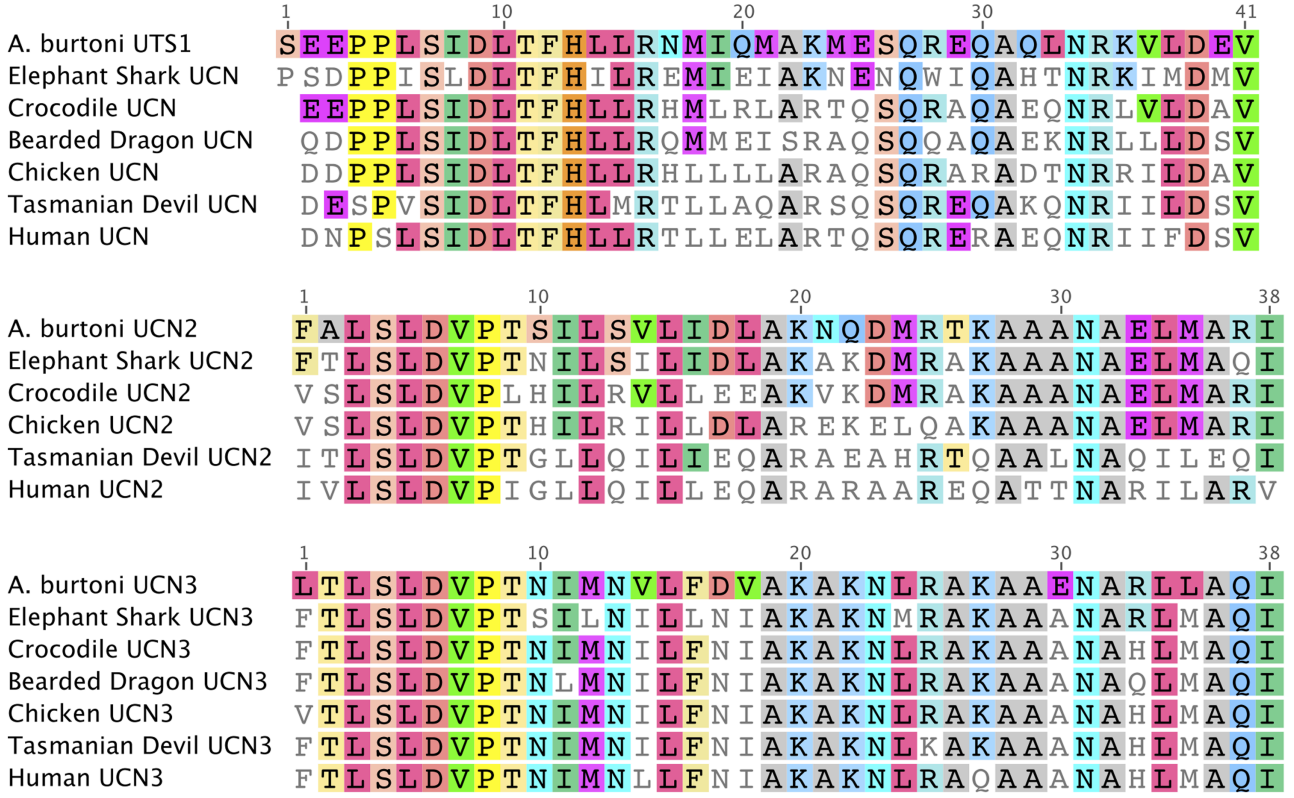

FIGURE 3 Predicted amino acid sequences for UCN, UCN2, and UCN3 processed peptides. Sequences were aligned using MAFFT. Residues matching the *A. burtoni* sequence are highlighted in color. No UCN2 was found for bearded dragon [Color figure can be viewed at wileyonlinelibrary.com]

FIGURE 4 Expression of *crh*-family transcripts in peripheral tissues of adult *A. burtoni*. Representative tissue distribution of transcripts is shown by PCR and gel electrophoresis from reverse transcribed cDNA. PCR products from *β-actin* transcripts in the same samples are shown below. Base pair (bp) numbers to the left are sizes of the indicated ladder bands while bp numbers in parentheses to the right of each gene represent the product size. A DNA ladder (100 bp ladder) is shown in the first lane

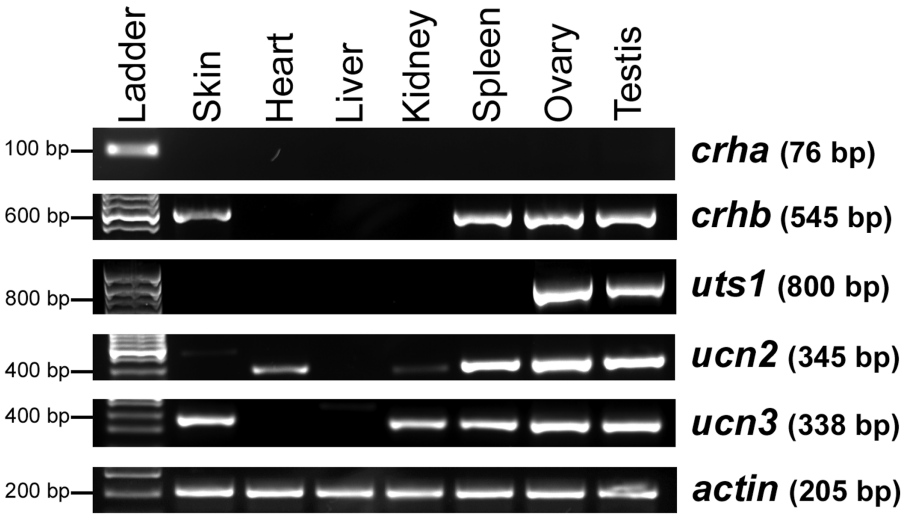

crhb populate the central and dorsal posterior thalamic nuclei (CP, DP) and occur in the area of the ventromedial thalamic nucleus (VMn) and the anterior glomerular nucleus (aGn) (Figures 7(f2–h2) and 8(e)). *crhb*-expressing cells lie along the midline in the paraventricular organ (PVO) and extend rostrally into the ventral periventricular nucleus of the posterior tuberculum (TPp) (Figure 8(e)). Several groups of *crhb*-expressing cells are found around the glomerular nucleus (Gn) in the lateral thalamic nucleus (LT), and the areas near dorsal preglomerular nucleus (PGd) and nucleus of the pretectoisthmic tract (nTPI) (Figure 7 (i2–j2)).

3.4.3 | Mesencephalon and rhombencephalon

Abundant *crhb* expression is found throughout the periventricular gray zone of tectum (PGZ) and multiple small groups of *crhb*-

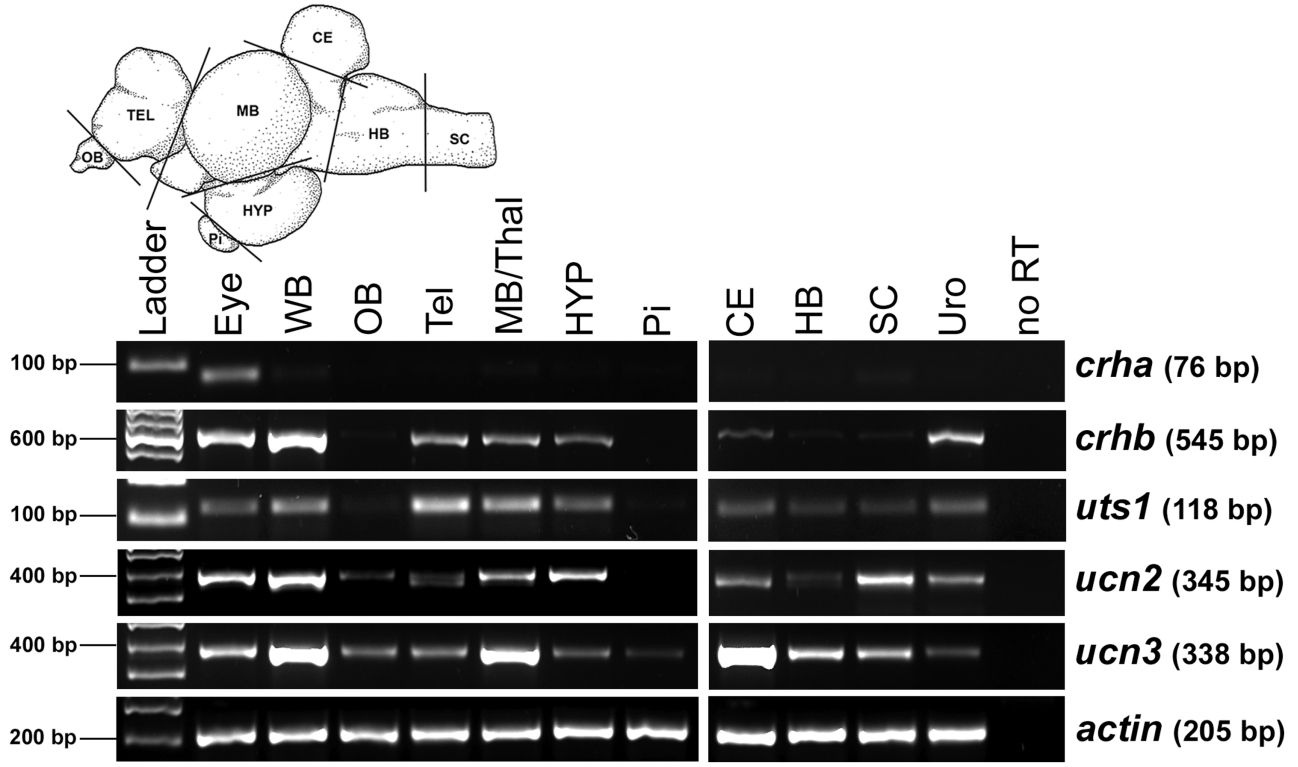

FIGURE 5 Expression of *crh*-family transcripts in macrodissected brain and nervous tissues of adult *A. burtoni*. Representative tissue distribution of transcripts is shown by PCR and gel electrophoresis from reverse transcribed cDNA. PCR products from *β-actin* transcripts in the same samples are shown below. Inset shows a sagittal view of the *A. burtoni* brain to illustrate the approximate macrodissection cuts used for analysis. A no reverse transcriptase (no RT) negative control and DNA ladder (100 bp ladder) are also shown. Base pair (bp) numbers to the left are sizes of the indicated ladder bands while bp numbers in parentheses to the right of each gene represent the product size. CE, cerebellum; HB, hindbrain; HYP, hypothalamus; MB/Thal, midbrain and thalamus; OB, olfactory bulb; Pi, pituitary; SC, spinal cord; TEL, telencephalon; Uro, urohypophysis; WB, whole brain

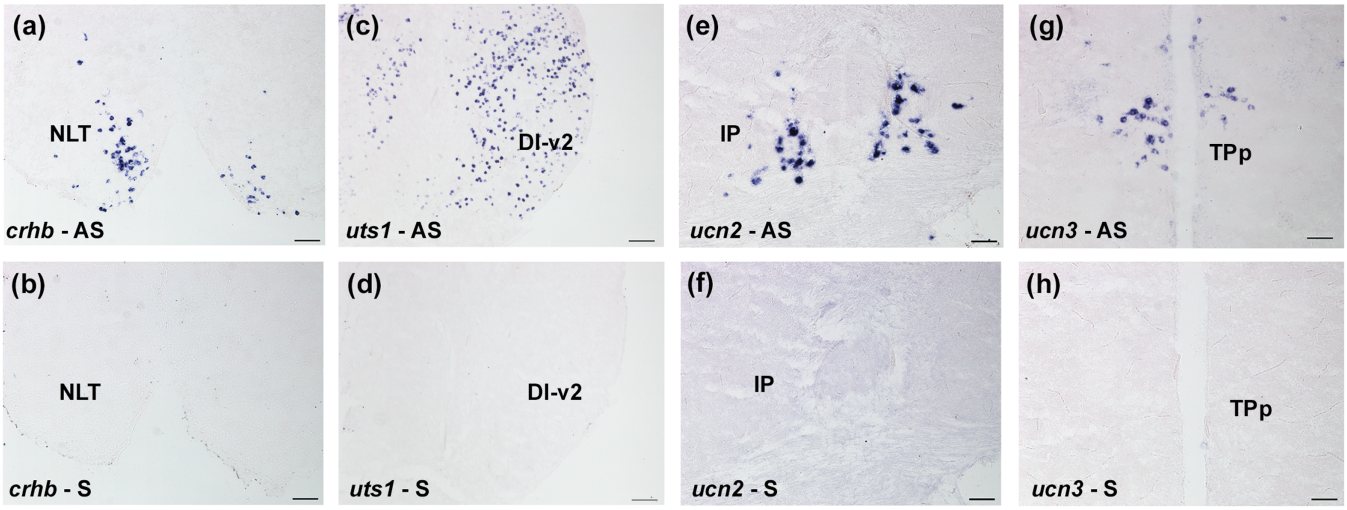

FIGURE 6 Representative examples of chromogenic in situ hybridization staining in the brain of *Astatotilapia burtoni* to show probe specificity. Antisense (AS) and sense (S) control probes are shown for *crhb* (a, b), *uts1* (c, d), *ucn2* (e, f) and *ucn3* (g, h). Photographs of AS and S were taken on alternate transverse sections from the same brain run simultaneously in the same ISH experiment. Sense control probes did not show any positive staining for any gene transcripts. See list for abbreviations. Scale bars = 50 μm (a, b, e, f, g, h); 100 μm (c, d) [Color figure can be viewed at wileyonlinelibrary.com]

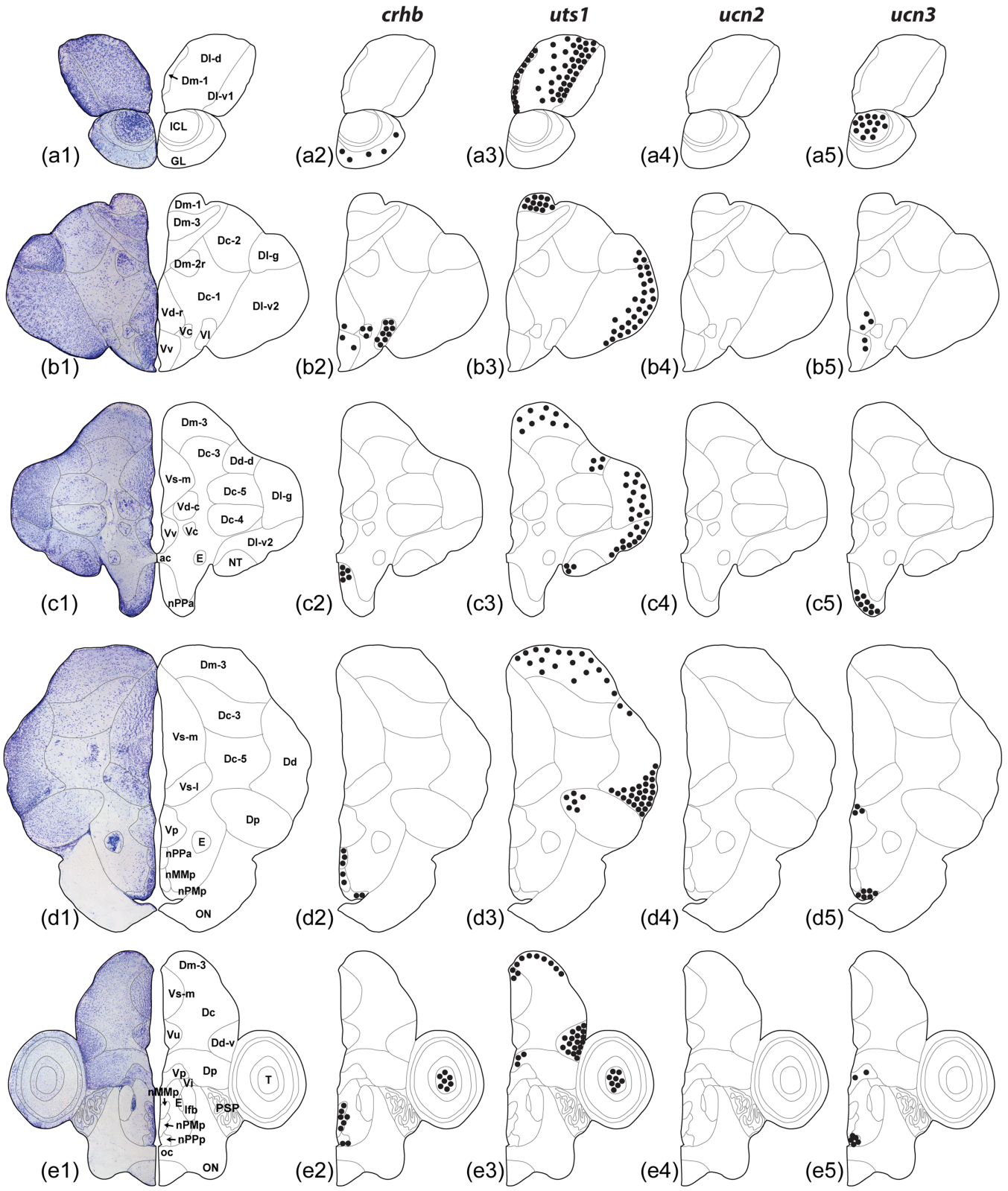

FIGURE 7 Summary of localization of *crhb*, *uts1*, *ucn2*, and *ucn3* throughout the brain of *A. burtoni*. Representative transverse sections are shown from rostral (a) to caudal (p). Left column in each row shows a transverse section stained with cresyl violet (left side) and a traced mirror image with nuclei and other neuroanatomical structures labeled (right side). Localization of cells (dots) expressing *crhb*, *uts1*, *ucn2* and *ucn3* are shown on traced images of the right side of each transverse section. See list for abbreviations [Color figure can be viewed at wileyonlinelibrary.com]

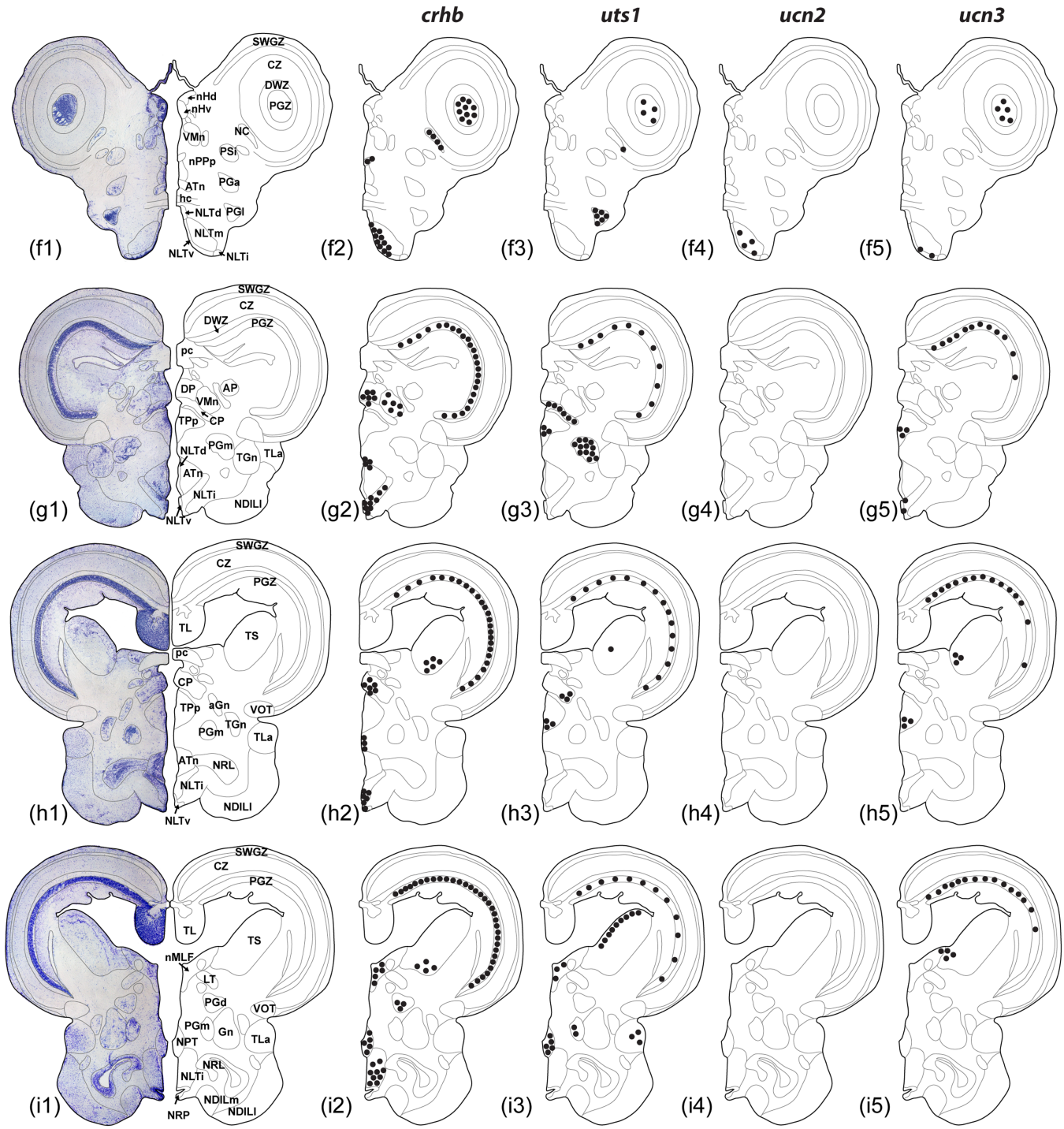

FIGURE 7 (Continued)

expressing cells are found in torus semicircularis (TS) (Figures 7(h2–l2) and 8(f)). One group contains smaller cells in the dorsal part of TS, possibly in central nucleus of TS (TSc), and a group of larger cells is found in the ventral TS, near the periaqueductal gray (PAG) (Figures 7(i2–k2) and 8(f)). Another group of *crhb*-expressing cells are found along the border between the ventrolateral nucleus of TS (TSvl) and the paratoral tegmental nucleus (PTT) (Figure 7(k2)). Large *crhb*-expressing cells are found in the nucleus of medial longitudinal fasciculus (nMLF) and oculomotor nucleus (IIIn) (Figures 7(i2–k2) and 8(f)).

A few large, darkly stained *crhb* cells are in the locus coeruleus nucleus (LC) and at the lateral border of the fourth ventricle (4v) in the central gray (CG) (Figures 7(l2–m2) and 8(g)). Scattered cells expressing *crhb* are in the medial and inferior reticular nuclei (Rm, Ri)

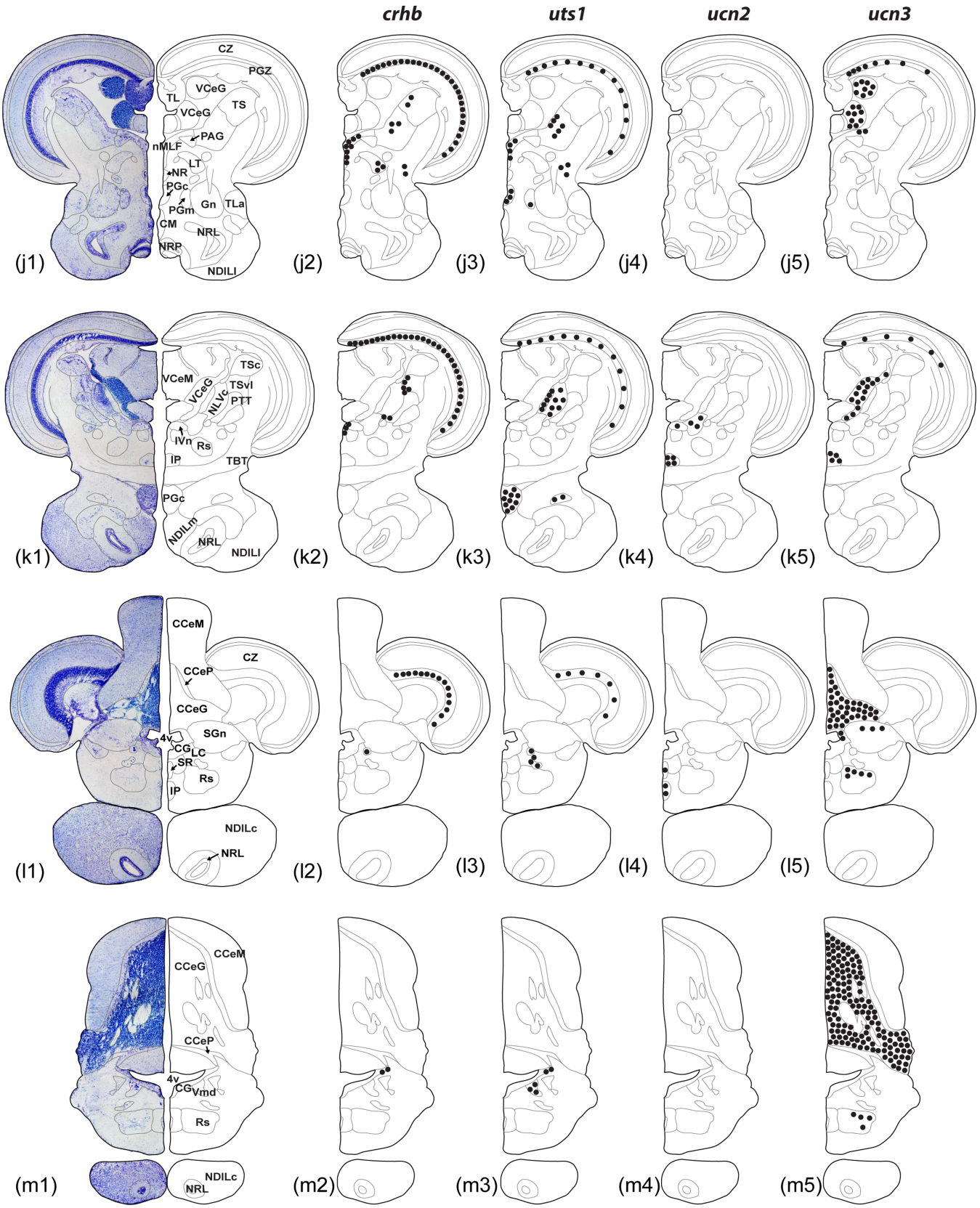

FIGURE 7 (Continued)

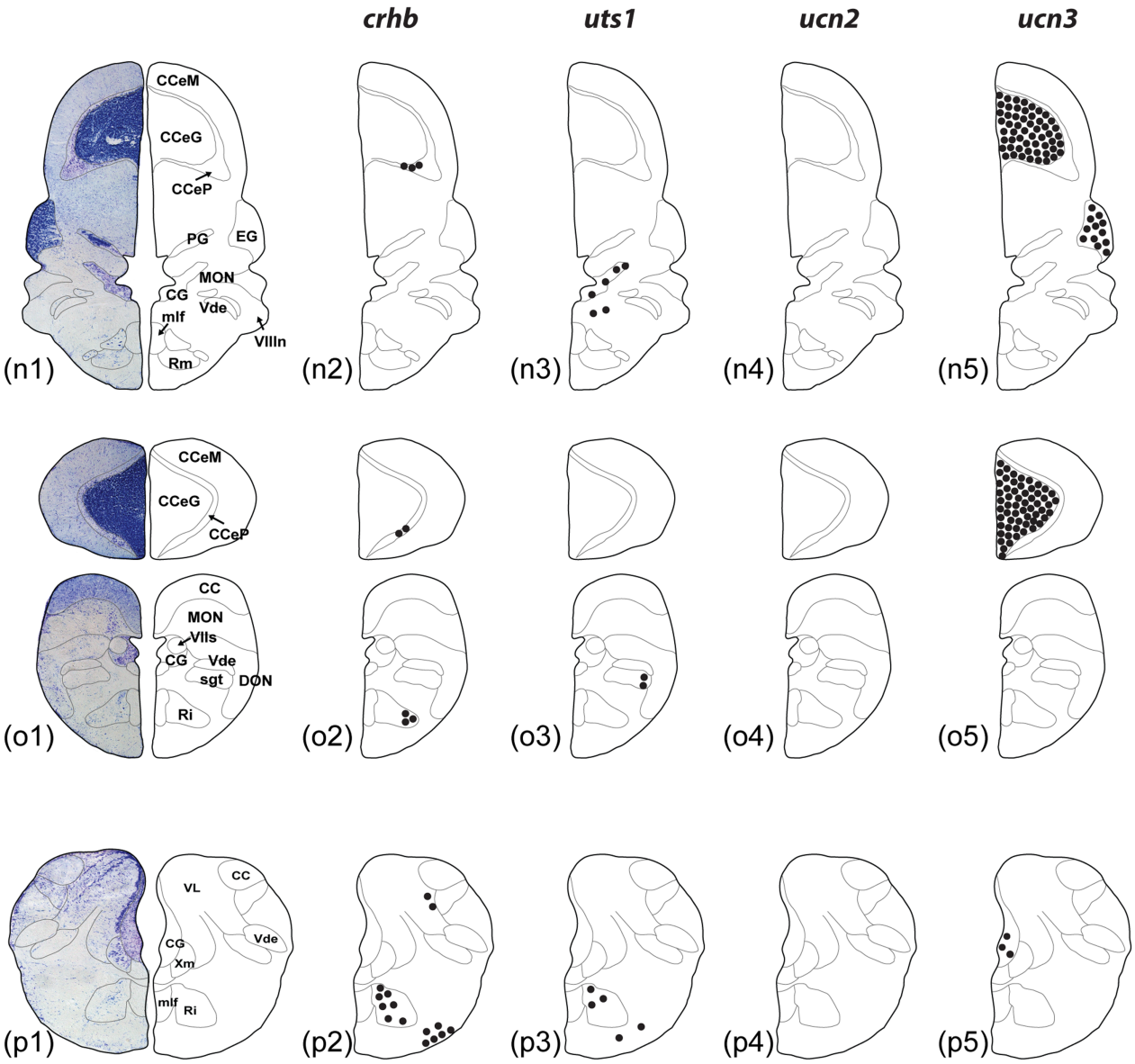

FIGURE 7 (Continued)

(Figures 7(o2–p2) and 8(h)), and possibly within Raphe nuclei. A few lightly stained *crhb*-expressing cells lie in the ventral Purkinje layer of corpus cerebellum (CCeP) (Figures 7(n2–o2) and 8(i)). Scattered *crhb*-stained cells are also found along the ventrolateral edge of the spinal cord (Figure 7(p2)).

3.5 | Localization of *uts1* expression

3.5.1 | Olfactory bulbs and telencephalon

Compared to *crhb* expression, *uts1* expression is much more widespread throughout the telencephalon, especially dorsal subdivisions (Figures 7(a3–e3) and 9(a–c)). No *uts1*-expressing cells were observed in the olfactory bulbs (Figure 7(a3)). Dense *uts1* staining lies along the medial edge of the rostral telencephalon in the medial part of the dorsal telencephalon, subdivision 1 (Dm-1) (Figures 7(a3) and 9(a)). Cells expressing *uts1* are also scattered throughout the dorsal part of lateral zone of the dorsal telencephalon (Dl-d) and along the lateral edge in the granular and ventral zones of lateral zone of the dorsal telencephalon (Dl-g, Dl-v) and of the dorsal part of the dorsal telencephalon (Dd) (Figures 7(b3-e3) and 9(a,b)). *uts1*-expressing cells are more abundant in the caudal Dd (Figure 7(d3–e3)). In the caudal telencephalon, *uts1*-expressing cells also populate the Dm-3 (Figures 7(c3-e3) and 9(c)). A few cells are located along the ventral edge of the Dl-v, subdivision 2 (Dl-v2), possibly in the nucleus taenia (NT) (Figure 7(c3)). Scattered cells are found the medial portion of posterior part of the dorsal telencephalon (Dp) (Figure 7(d3–e3)).

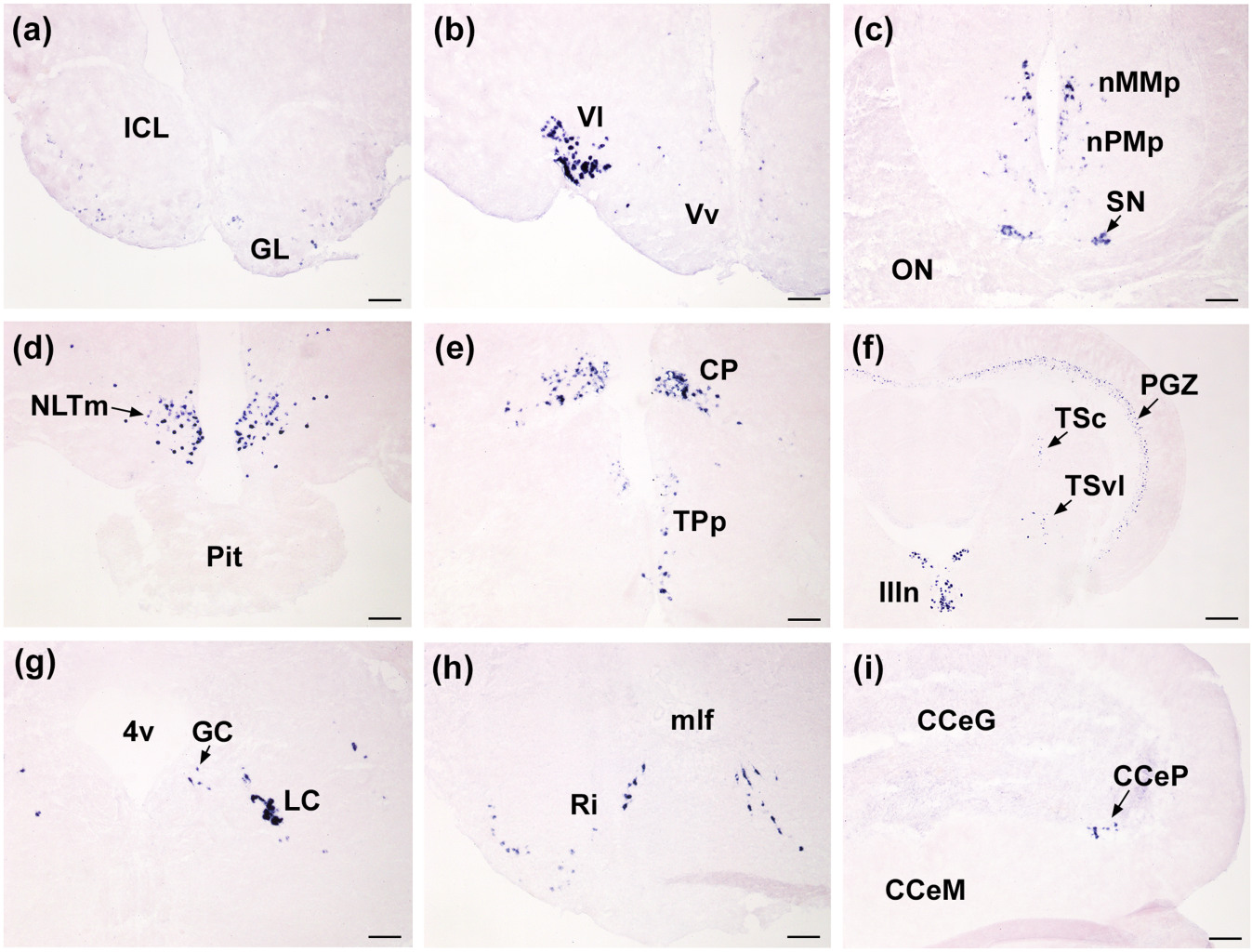

FIGURE 8 Representative photomicrographs of *crhb*-expressing cells in the brain of *A. burtoni*. A few scattered *crhb*-expressing cells lie in the glomerular layer of the olfactory bulbs (a). A large densely stained *crhb* cell population exists in Vl (b). Several nuclei within the preoptic area (c), the SN, and the NLT (d) contain *crhb*-expressing cells. *crhb*-expressing cells occur in CP and TPp (e). In the midbrain, *crhb*-expressing cells are scattered in the torus semicircularis, and abundant throughout the PGZ of the tectum (f). Large cells in IIIn also express *crhb* (f). In more caudal sections, *crhb*-expressing cells lie in CG around the 4th ventricle and in LC (g), and in nuclei of the reticular formation (h). Some Purkinje cells in the cerebellum also express *crhb* (i). Photomicrographs were taken from 20 μm transverse sections. Scale bars = 100 μm (a, b, c, d, e, g, h, i); 250 μm (f). See list for abbreviations [Color figure can be viewed at wileyonlinelibrary.com]

3.5.2 | Diencephalon

No *uts1*-expressing cells are found in the POA (Figure 7(c3–f3)). A population of *uts1*-expressing cells are found throughout the thalamic CP, more lateral to where *crhb*-expressing cells were located (Figures 7(g3-h3) and 9(d)). A few *uts1* cells lie in the ventral part of NC (Figure 7(f3)). The TPp also contains a group of *uts1*-expressing cells (Figure 7 (g3–h3)). *uts1* expression is found throughout the preglomerular complex, especially in the lateral preglomerular nucleus (PGl), medial preglomerular nucleus (PGm), and, more caudally, in the commissural preglomerular nucleus (PGc) (Figures 7(f3–g3,i3) and 9(d,e)). Like *crhb*, a few large *uts1*-expressing cells are found along the midline in the nMLF and IIIn (Figures 7(i3-j3) and 9(g)). Some scattered cells are found in the nucleus of the torus lateralis (TLa) and in NPT (Figure 7 (i3)). Like *crhb*, a group of *uts1*-expressing cells is found dorsolateral to the Gn and in LT (Figures 7(i3–j3) and 9(e)).

3.5.3 | Mesencephalon and rhombencephalon

Like *crhb*, *uts1* is expressed throughout the PGZ layer of the tectum (Figures 7(e3–l3) and 9(h)). Density of cells expressing *uts1* in this region appears lower than *crhb* but becomes denser more caudally. Cells expressing *uts1* are also found in the TSvl, especially along the edge of PTT, in the PTT, and in the NLV regions along the ventricle (Figures 7(j3–k3) and 9(f)). Some small *uts1*-expressing cells are also scattered in the area of the dorsal tegmental nucleus (DT). A few large, darkly stained *uts1* cells are found in the caudal LC (Figure 7(l3)) and

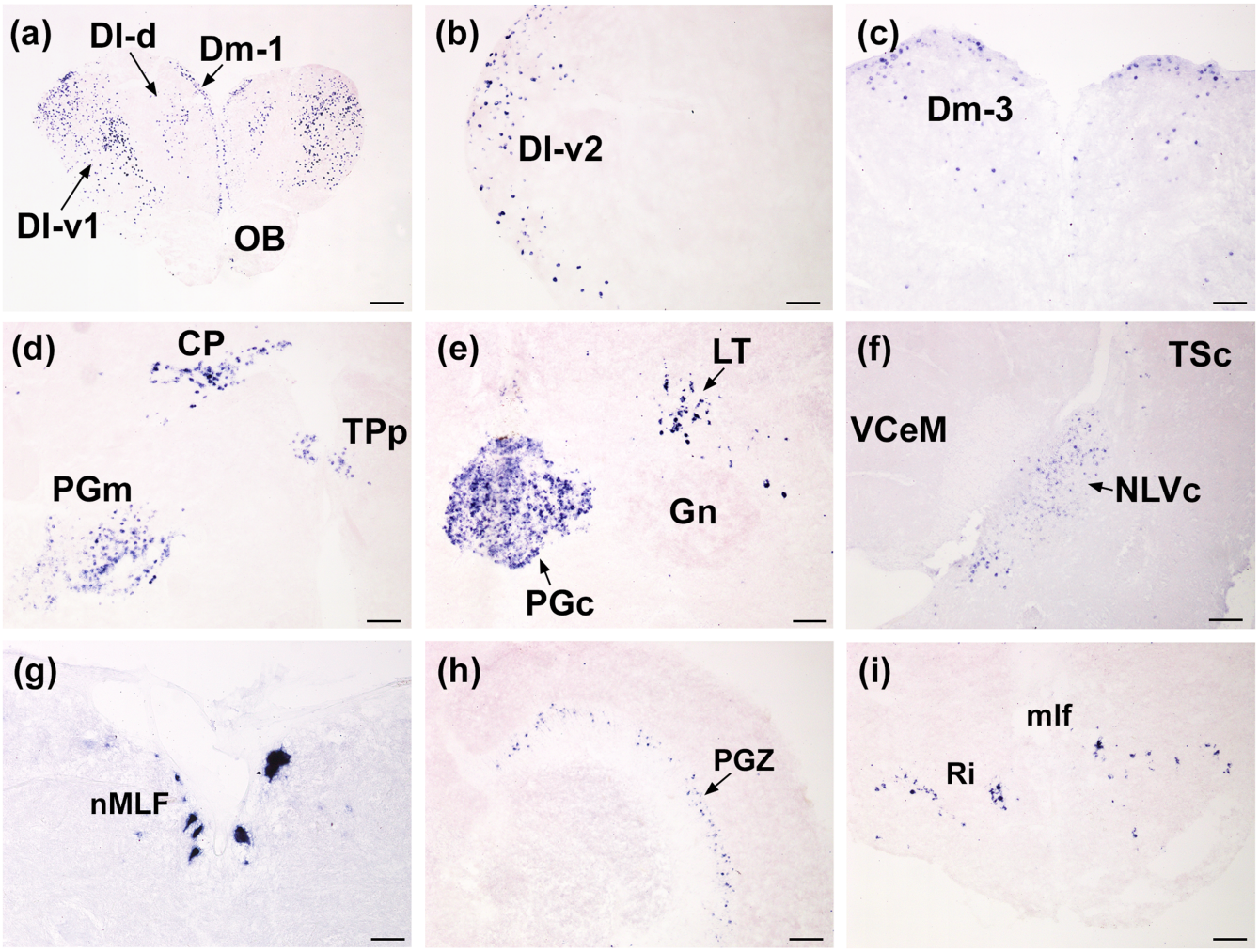

FIGURE 9 Representative photomicrographs of *uts1*-expressing cells in the brain of *A. burtoni*. *uts1*-expressing cells are abundant in rostral regions of the dorsal telencephalon including Dl-d, Dm-1, and Dl-v1 (a), as well as Dl-v2 (b) and Dm-3 (c) more caudally. In the diencephalon, uts1-expressing cells like in CP, PGm, and TPp in rostral sections (d), and in PGc and LT caudally (e). Small scattered cells are present in NLVc (f), and large cells lie in nMLF (g). In the tectum, *uts1*-expressing cells are abundant throughout the PGZ (h). Cells are also present in the reticular nuclei of the hindbrain (i). Photomicrographs were taken from 20 μm transverse sections. Scale bars = 250 μm (a); 100 μm (b, c, d, e, f, h, i); 50 μm (g). See list for abbreviations [Color figure can be viewed at wileyonlinelibrary.com]

preeminential nucleus (PE), and become denser more caudally. Similar to *crhb*, a few large cells are found at the lateral borders of 4v in CG, scattered throughout the CG, and just ventral to CG (Figure 7(l3–n3)). Several large *uts1*-expressing cells are located in dorsal motor nucleus of trigeminal nerve (Vmd) (Figure 7(m3)) and facial nerve (cranial nerve VII; VIIn). *uts1*-expressing cells are scattered throughout Ri and along the brain edge just ventral to Ri (Figures 7(n3–p3) and 9(i)i).

3.6 | Localization of *ucn2* expression

Compared to the other *crh*-family genes, *ucn2* expression is more restricted (Figure 7(f4, k4, l4)). Scattered cells lie in several subdivisions of the rostral NLT (NLTi, NLTv) in some but not all animals (Figures 7(f4) and 10(a)). Cells expressing *ucn2* are found in the region of the trochlear nucleus (IVn) and DT (Figures 7(k4) and 10(b)), and in the interpeduncular nucleus (IP) (Figures 7(k4–l4) and 10(c)). Some scattered cells may also extend into Raphe nuclei along the midline and anterior to the region of IP (Figure 7(l4)).

3.7 | Localization of *ucn3* expression

3.7.1 | Olfactory bulbs and telencephalon

ucn3-expressing cells lie in the olfactory bulbs and are most abundant in the internal cell layer (ICL) (Figures 7(a5) and 11(a)). Scattered *ucn3*-expressing cells are also found in Vv and Vd but more lateral than the *crhb*-expressing cells in these areas (Figures 7(b5) and 11(b)). A few cells stained for *ucn3* occur in the area between the supracommissural and postcommissural parts of the ventral telencephalon (Vs, Vp), and within the caudal Vp (Figure 7(d5–e5)).

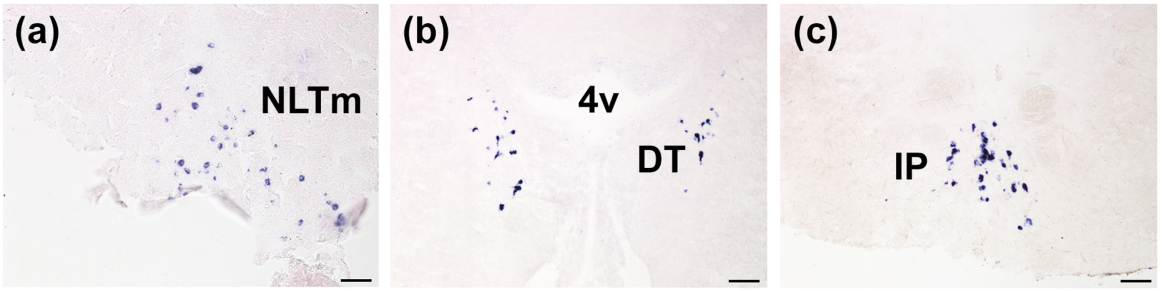

FIGURE 10 Representative photomicrographs of *ucn2*-expressing cells in the brain of *A. burtoni*. Scattered cells are found in the diencephalic NLT (a), midbrain DT (b), and hindbrain IP (c). Photomicrographs were taken from 20 μm transverse sections. Scale bars = 50 μm (a); 100 μm (b, c). See list for abbreviations [Color figure can be viewed at wileyonlinelibrary.com]

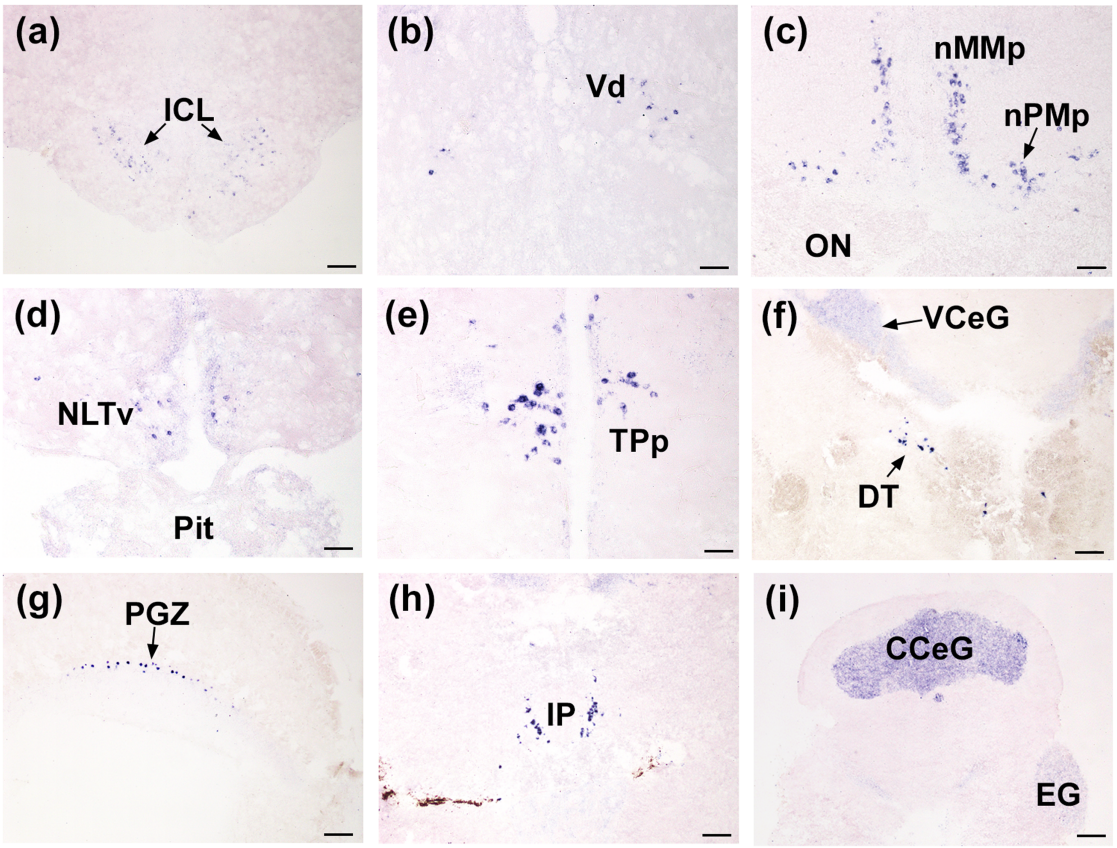

FIGURE 11 Representative photomicrographs of *ucn3*-expressing cells in the brain of *A. burtoni*. Cells lie in the inner cellular layer of the olfactory bulbs (a), and a few scattered cells are seen in Vd (b). *ucn3*-expressing cells are found throughout preoptic nuclei (c) and scattered in the NLT (d). Cells are also present in the TPp (e) and DT (f). In the tectum, *ucn3*-expressing cells lie in the PGZ, primarily in the dorsal region **(g).** In the hindbrain, cells lie in IP (h), and the granular regions of the corpus and valvulae cerebelli show dense *ucn3* staining (f,i). Photomicrographs were taken from 20 μm transverse sections. Scale bars = 100 μm (a, f, g, h, i); 50 μm (b, c, d, e). See list for abbreviations [Color figure can be viewed at wileyonlinelibrary.com]

3.7.2 | Diencephalon

Only small, parvocellular-like cells were stained for *ucn3* in nuclei of the preoptic area (Figures 7(c5–e5) and 11(c)). Staining was present in the nPPa, but more ventral to that observed for *crhb* (Figure 7(c5)). In addition, *ucn3*-expressing cells were found in the nPMp, nMMp, and parvocellular preoptic nucleus, posterior part (nPPp) divisions of the POA (Figure 7(d5–e5)). A few scattered cells also lie in the rostral portion of NLTv (Figures 7(f5–g5) and 11(d)). A group of *ucn3* cells are found in the TPp in a similar position as *uts1*-expressing cells (Figures 7(g5–h5) and 11(e)), and some scattered cells lie in the region of NPC lateral to habenular nuclei.

3.7.3 | Mesencephalon and rhombencephalon

Similar to *crhb* and *uts1*, *ucn3* expression is found in the PGZ of the tectum (Figures 7(f5–k5) and 11(g)). Staining was denser than *uts1*, but not as dense as *crhb*, and was more abundant in the rostral and medial tectum. Cells were also more abundant in the dorsal PGZ throughout its extent compared to lateral and ventral regions (Figure 7(g5–k5)). A group of large *ucn3*-expressing cells are found in the area near PAG (Figure 7(j5)). Expression of *ucn3* in the IP is similar to that of *ucn2* (Figures 7(k5) and 11(h)). Like *uts1*, a few *ucn3*-expressing cells are found along the ventricle border in the region of DT (Figure 11(f)). Granular cell-like *ucn3* staining is found throughout the granular layers of corpus cerebellum (CCeG), valvulae cerebellum (VCeG), and within the eminentia granularis (EG) (Figures 7(j5–o5) and 11(f,i)). This expression is supported by a strong band present in RT-PCR of the cerebellum (see Figure 5). A few large *ucn3*-expressing cells are found along the 4v border in CG, which extends caudally to the spinal cord (Figure 7(p5)), and throughout the dorsal secondary gustatory nucleus (SGn) (Figure 7(l5)). Some *ucn3*-expressing cells are scattered throughout the superior reticular nucleus (Rs) (Figure 7(l5–m5)).

4 | DISCUSSION

Here, we provide phylogenetic analysis, tissue expression, and brain localization patterns for the suite of CRH-family genes in a single teleost species. Our phylogenetic analysis of *A. burtoni* CRH-family peptides confirmed that *crha* and *crhb* are closely related and form a clade with *uts1*, while *ucn2* and *ucn3* are in a separate group. While *crhb*, *uts1*, and *ucn3* are found in several body tissues and are widespread throughout the brain, *crha* and *ucn2* show more restricted expression patterns. A broader phylogenetic analysis of UCNs also identified novel UCN2 homologs in reptiles, which have not been previously shown to possess UCN2. Our searches found no UCN2 in some reptiles, suggesting a potential loss in snakes and lizards. The absence of UCN2 genes in lizards is similar to the lack of known UCN2 in frogs (Boorse et al., 2005), suggesting reduced constraints on the evolution of these peptides in some lineages. Collectively, our results provide insights into the molecular evolution and diverse functions of the CRH gene family across vertebrates.

4.1 | Evolutionary origins

We cannot make sense of any part of the biology of CRH peptides, except in the light of evolution (Dobzhansky, 1973). CRH homologs are present in many invertebrates as well as in all vertebrates, indicating an ancient evolutionary origin for this family of peptides. CRH-like diuretic hormone (DH44) genes are found in insects, first described in the moth *Manduca sexta* (Kataoka et al., 1989) and subsequently in many other insect species (Cabrero et al., 2002; Cardoso et al., 2014). Insect DH44 stimulates fluid secretion via cyclic AMP signaling. In *Drosophila melanogaster*, DH44 is expressed in neuroendocrine cells of the pars intercerebralis (Cabrero et al., 2002). The homeostatic function of insect CRH homologs is functionally reminiscent of the fluid homeostasis functions of vertebrate CRH orthologs, suggesting a potentially conserved ancestral function. CRH homologs are also found in annelids, nemerteans, mollusks, and arthropods, with differing gene numbers suggesting independent duplications in some lineages (De Oliveira et al., 2019). The gastropod CRF/DH44-like egg-laying hormone (ELH) genes, initially isolated from *Aplysia californica*, inhibit feeding and stimulate ovulation (Chiu et al., 1979). In general, ancestral roles of the CRH family peptides, in invertebrates as well as vertebrates, are hypothesized to include regulation of feeding and diuresis (Lovejoy et al., 2014).

Prior to the identification of CRH2 as a second vertebrate CRH gene, two distinct models of vertebrate CRH-family evolution were proposed. Lovejoy and colleagues suggested that a single ancestral peptide gene in a vertebrate progenitor was duplicated during two rounds of whole-genome duplication, giving rise to two pairs of related peptides: CRH/UCN and UCN2/UCN3 (Lovejoy & de Lannoy, 2013). The finding of a single CRH-like peptide in tunicate species was consistent with this model (D'Aquila et al., 2016). An alternative model posits that separate CRH/Ucn (UI)-like and Ucn2/3-like paralogous lineages arose prior to the evolution of agnathans. A "sub-genomic event" then led to a split between CRH and UTS lineages. After the jawed vertebrates diverged from agnathans, UCN2 and UCN3 diverged. This model is supported by the location of *CRH1*, *CRH2*, and *UCN1* genes in a proposed paralogon with opioid peptide and receptor genes, while UCN2 and UCN3 are located in a paralogon that also contains visual opsin and oxytocin/vasopressin receptor genes (Cardoso et al., 2016). However, the genes located in syntenic blocks with UCN2 are not closely homologous to genes in synteny with UCN3, and the paralogon analysis relies on comparisons of genes that are distant from each other in large chromosomal regions. Although three CRH family members are identified in the sea lamprey, *Petromyzon marinus* (Endsin et al., 2017), the implications of lamprey genes for understanding CRH family evolution are limited by uncertainties about the timing of vertebrate whole-genome duplications relative to agnathan evolution (Holland & Ocampo Daza, 2018) and by the extensive genomic evolution of modern lampreys compared to any ancestral agnathans, including potential duplications and gene loss.

Altogether, the balance of the currently available evidence appears consistent with a scenario in which an ancestral CRH-like gene was duplicated preceding two rounds of vertebrate whole-genome duplication. However, there are remaining uncertainties about the exact timing of the origins of the five vertebrate CRH paralogs. Even more importantly, it is not yet understood why these duplicated genes were retained, or how their functions evolved in different lineages.

4.2 | Comparative neuroanatomy of vertebrate CRH, UTS1, UCN2, and UCN3 and functional implications

Our ISH staining in *A. burtoni* revealed widespread distribution of *crhb* cells from the olfactory bulbs to the hindbrain. Previous reports also document broad expression of CRH genes in the brains of several

vertebrates, including mammals and some fishes. For many years, only the *crhb* genes were studied in teleosts, because *crha* had not yet been identified. In teleosts, the primary location of hypophysiotrophic *crhb* neurons is the preoptic area. These neurons have been studied with immunohistochemistry in several teleost species including chinook salmon, white sucker, and brown ghost knifefish (Matz & Hofeldt, 1999; Yulis et al., 1986; Zupanc et al., 1999). In tilapia, an African cichlid fish closely related to *A. burtoni*, many cell bodies were located in the ventral telencephalon, with dense CRH-immunoreactive terminals in the rostral dorsal telencephalon (Pepels et al., 2002). Other tilapia CRH neuron populations were located in the preoptic area, tuberal region, olfactory bulb, and optic tectum, similar to the *crha* expression pattern observed here in *A. burtoni*. A cluster of dorsally-projecting, ventrally located CRH-immunoreactive neurons was also observed in the sailfin molly, *Poecilia latipinna* (Batten et al., 1990). In another poecilid fish, *Gambusia affinis*, CRH-ir was observed in ventral telencephalon in addition to POA and NLT cell populations (Coto-Montes et al., 1994). In gilthead bream, *Sparus aurata*, CRH-ir neurons were largely absent from the POA, but prominent in NLT (Mancera & Fernández-Llebrez, 1995). Populations of hypothalamic *crhb* neurons in *A. burtoni* hypothalamus likely share developmental homologies with other vertebrates, for example, the *otpa*-expressing neurons that give rise to neuropeptidergic cells in the supraoptoparaventricular region of zebrafish (Biechl et al., 2017). Overall, several teleost fish species are known to express *crhb* in a variety of regions in addition to the prominent preoptic area cell cluster. The teleost localization patterns within nuclei homologous to those in tetrapods suggests some conservation of function in homeostatic processes including stress regulation, feeding, anxiety, and behaviors.

In *A. burtoni*, *crhb*, along with *uts1* and *ucn3*, was expressed to some extent in several sensory processing regions such as the olfactory bulbs, thalamic nuclei, tectum, torus semicircularis, and secondary gustatory nucleus. Similarly, CRH-related peptides, and particularly CRH itself, are also found in central sensory processing regions of mammals (Imaki et al., 1991; Lim et al., 2006; Potter et al., 1992). This raises the possibility of conserved modulatory functions in olfaction, vision, and hearing abilities possibly related to stress, fear, and anxiety responses via connections with limbic circuitry. In *Xenopus*, for example, CRF neurons in the visual tectum help modulate food intake in the presence of certain stressors (Prater et al., 2018), and CRF plays a role in acoustic startle responses in mammals via circuitry that includes auditory pathways and the amygdala (Risbrough et al., 2003). While there is limited information on whether Crf plays a role in sensory processing in fishes, a study in zebrafish demonstrated that the brain Crf system is essential for regulating innate camouflage behavior in response to light versus dark conditions (Wagle et al., 2011). The widespread distribution of *crhb* in the vertebrate brain and its diverse roles in many behaviors and physiological functions suggests it plays important roles in modulating the circuitry linking sensory inputs to behavioral decisions.

Reports of *crha* expression are very limited thus far. In this study, our RT-PCR results supported our previous finding that *crha* is exclusively expressed in *A. burtoni* eye, without detectable levels in other tissues. Expression of *A. burtoni crha* in the retina and its absence in the brain was initially demonstrated using in situ hybridization (Grone & Maruska, 2015a). Medaka *crha* (also referred to as teleocortin) expression was reported in all peripheral tissues that were tested, but at low levels compared to a control gene, *eef1a* (Hosono et al., 2015). The highest expression level was detected in the medaka eye. In grass carp, *crha* was detected in the brain, along with *crhb*, *uts1*, and *ucn3*, but more detailed analyses of expression patterns in the carp brain were not reported (Ye et al., 2019). Until additional species are examined, it remains unclear how much diversity in *crha* expression and function may exist.

Cells expressing *uts1* were widely distributed throughout the entire *A. burtoni* brain, often with co-regionalization in the same nuclei as other CRH-family genes. UCN1/UTS1 distribution has been studied in a range of vertebrate species, including several mammals as well as fishes. In mammals, UCN1 is expressed in several regions of the brain, including prominent expression in the centrally projecting peptidergic Edinger–Westphal nucleus (EWcp) (Kozicz et al., 2011). The urocortin-expressing EW cells have diverse projections within the central nervous system, and likely functional roles in stress adaptation and food intake, as reviewed in the study by Kozicz et al. (2011). Zebrafish have an Edinger–Westphal nucleus (Mueller et al., 2004), located lateral to the nucleus of the medial longitudinal fasciculus (nMLF) but *uts1* expression in this region has not been verified. In *A. burtoni*, we identified a population of large cells near the nMLF that strongly expressed *uts1* mRNA. Given the prominence and location of this staining, it is possible that these *uts1*-expressing neurons are functionally homologous to the mammalian *Ucn1*-expressing EW cells.

Similar to the broad distribution of *Ucn1* in tetrapod brains, we found many nuclei expressing *uts1* throughout the *A. burtoni* brain. In human brain, UCN1 mRNA and protein were detected broadly, including hypothalamus, pons, cerebral cortex, and cerebellum (Takahashi et al., 1998). Rat UCN1 expression was investigated via immunohistochemistry (Kozicz et al., 1998; Morin et al., 1999), which revealed expression in hypothalamic, raphe, and tegmental nuclei, in addition to extensive labeling in the Edinger–Westphal nucleus. A study of voles using in situ hybridization revealed expression mainly in the Edinger–Westphal nucleus (Lim et al., 2006). In the green frog, *Rana esculenta*, cell bodies with UCN1-like immunoreactivity were detected in several nuclei of the telencephalon, diencephalon, mesencephalon, and rhombencephalon, with prominent staining in the Edinger–Westphal nucleus (Kozicz et al., 2002).

Among teleosts, *uts1* expression was previously examined in medaka and zebrafish brains. Medaka *uts1* expression is observed in telencephalon, thalamus, and brainstem (Hosono et al., 2017). Zebrafish *uts1* mRNA expression was observed in developing hypothalamus, as well as nuclei of the telencephalon, diencephalon, hindbrain, and spinal cord (Alderman & Bernier, 2007; Brautigam et al., 2010). Generally, *uts1* distribution in *A. burtoni* is very similar to that seen in zebrafish, but some differences with medaka are evident. For example, we observed *uts1* cell populations in several mesencephalic regions, including the tectum and torus semicircularis, and hindbrain regions, neither of which are described in medaka. It is difficult to ascertain possible functional consequences of this *uts1* expression until additional species are examined.

The functions of Ucn2 and Ucn3 peptides depend on their expression patterns, as well as their ability to selectively bind CRF Receptor 2 (Reyes et al., 2001). In mammals, *Ucn2* mRNA is found in several brain regions including hypothalamus, supraoptic nucleus, and spinal trigeminal nucleus. In zebrafish, *ucn3* mRNA was detected in developing embryos from 24 hours onwards, in hindbrain rhombomeres 2 and 4, the superior raphe nucleus, optic tectum, telencephalon, and the retina (Brautigam et al., 2010). In *A. burtoni*, *ucn2* showed very restricted distribution in the brain, while *ucn3* was relatively more widespread and abundant. This overall pattern is similar to that seen in the medaka brain (Hosono et al., 2017). Expression of *ucn2* in medaka brain was restricted to VM in the thalamus and NIP and raphe nucleus in the brainstem, with weak expression also seen in NDLI of the hypothalamus (Hosono et al., 2017). In contrast, medaka *ucn3* was detected in many regions of the brain including nuclei in the ventral telencephalon, preoptic area, thalamus, hypothalamus, optic tectum, and brainstem. Localization of *ucn2* and *ucn3* in the interpeduncular nucleus of *A. burtoni* supports the possibility, proposed for medaka, that these IP neurons function in experience-dependent modification of fear responses and regulation of social aggression in teleosts (Hosono et al., 2017). One unique feature of *ucn3* is its abundant expression in the cerebellum of *A. burtoni* revealed by both RT-PCR and ISH. Cerebellum *ucn3* expression is also seen in medaka (Hosono et al., 2017) and developing chick embryos (Grommen et al., 2017), but not in zebrafish or mammals (Brautigam et al., 2010; Lewis et al., 2001). It is possible that *ucn3* in some vertebrates has taken on functions in cerebellar-mediated motor performance, but this requires further study. In the medaka spinal cord, *ucn2* expression was observed in the ventral region, while *ucn3* expression was found in the dorsomedial region. The authors speculated that *ucn2* may be undergoing a loss of function in medaka. Relative to other peptides in the family, the fish *ucn2* sequences are highly divergent and the expression is restricted to a few nuclei.

Another way to view the current situation would be to suppose that the medaka *ucn2* has experienced some degree of subfunctionalization, which may allow *ucn2* to continue to perform specific adaptive functions in the context of medaka ecology and physiology. However, the sequence divergence and the apparent loss of *ucn2* in other fishes (such as zebrafish) and mammals does support the idea that evolutionary constraints on *ucn2* have been weakened, relative to *ucn3*. This difference between *ucn2* and *ucn3* is comparable to the relationship between the highly conserved *CRH1* gene and *CRH2*, which has diverged greatly in sequence, been lost multiple times in vertebrate evolution, and maintains a very restricted expression pattern in spotted gar (Grone & Maruska, 2015b). Nevertheless, the widespread central distribution of *ucn3* in both fishes and mammals suggests involvement in diverse and conserved physiological functions that include homeostasis and stress regulation. In mammals, Ucn3 peptide also has anorexigenic effects and was proposed to have a conserved role in inhibition of feeding (P. Chen et al., 2012; Fekete et al., 2007). Similarly, intraperitoneal injection of UCN3 into Siberian sturgeons inhibits food intake and may interact with CCK to cause anorexigenic effects as part of a brain-gut axis (Tang et al., 2019). In *A. burtoni* and the few other fishes examined, *ucn3* is also localized to regions implicated in food intake and metabolism such as POA and NLT (homolog of arcuate nucleus). Thus, *ucn3* may play a role in feeding regulation, but its broad expression patterns in other brain regions also suggests additional functions yet to be revealed.

4.3 | CRH/UCN expression and roles in peripheral tissues

CRH and Urocortin transcripts and peptides are identified in many tissues outside the brain across vertebrate taxa, highlighting the global importance of the CRH-family to physiological processes. In mammals, for example, several peripheral tissues express some combination of *Crf*, *Ucn1*, *Ucn2*, and *Ucn3*. Those tissues include ones that we examined in *A. burtoni*: skin, heart, liver, kidney, and spleen (Kageyama et al., 1999; Kimura et al., 2002; A. Slominski et al., 2000; Takahashi et al., 2004). There is substantial variety in tissue expression among different mammalian species. For example, mice differ from humans and even from rats in the complement of peptides expressed in the skin (A. T. Slominski et al., 2013).

This diversity of peripheral tissue expression patterns also seems to hold true for the limited nonmammalian taxa examined. We found that *A. burtoni* skin contains *crhb* and *ucn3* mRNA, in contrast to the skin of another cyprinid fish, *Schizothorax prenanti*, which did not contain detectable levels of *crhb* mRNA (Wang et al., 2014). *Ucn3* was, however, found in skin of *Xenopus laevis* (Boorse et al., 2005). Mammalian skin cells express a range of neuropeptides, hormones, and receptors, including CRH and Urocortin (A. T. Slominski et al., 2013). CRH peptides are expressed in the skin in response to inflammatory stressors and disease, and regulate skin cell proliferation, differentiation, immune functions, and secretory activity. If the proliferative and immune pathways are conserved across many teleosts, perhaps other CRH-family peptides serve similar functions in the skin in a range of fish species.

Our results show that *A. burtoni* heart does not express *uts1* or *ucn3* but does express *ucn2*. In zebrafish heart, mRNA encoding *crha*, *crhb*, *uts1*, and *ucn3* were detected (with *uts1* at the lowest levels), in addition to receptors and binding protein expression (Williams et al., 2017). Furthermore, hypoxia-reperfusion exposure increases *crhb* and *ucn3* expression in the zebrafish heart, and rat/human CRH and mouse UCN3 peptides were protective against hypoxia-induced apoptosis in zebrafish (Williams et al., 2017). CRH and Urocortin peptides have similar protective functions in mammalian heart (Davidson et al., 2009). In *Xenopus*, the heart expresses *ucn1* and *ucn3*, but a *ucn2* ortholog was not identified in this species (Boorse et al., 2005). The conserved role of this family of peptides in mammals and zebrafish suggests that *ucn2* might also serve some protective role in *A. burtoni* heart.

In *A. burtoni* spleen, we detected *crhb*, *ucn2*, and *ucn3* expression. This expression is reminiscent of rodent spleen, where both *Crf* (Aird et al., 1993) and *Ucn* (Kageyama et al., 1999) are expressed, although at relatively low levels. In mammals, CRH and

UCN likely modulate the peripheral immune response via various cell types, including spleen lymphocytes (Baigent, 2001). To date, the effects of CRH-family peptides in spleen do not appear well studied in any teleost species. In *A. burtoni* kidney, we detected *ucn2* and *ucn3*. Similarly, all three urocortin genes are found in mammalian kidneys, where they may regulate diuresis and improve renal function (Devetzis et al., 2013). In *Xenopus*, both urocortins identified in this species, *ucn1* and *ucn3*, are also detected in kidney (Boorse et al., 2005). In common carp, abundant CRH was detected in head kidney (Huising et al., 2007). The teleost head kidney, homologous to the mammalian adrenal gland, contains interrenal catecholamine-producing and glucocorticoid-producing cells, which play important roles in immune function and stress adaptation. While we only examined kidney and not head kidney in *A. burtoni*, the expression of both *ucn2* and *ucn3* in this tissue suggests diverse functional roles but requires further study.

In *A. burtoni* ovaries and testes, we detected *crhb*, *uts1*, *ucn2*, and *ucn3*. Human ovaries express both *CRH* and *UCN* mRNA (Florio et al., 2004). Strong expression of *Ucn1* mRNA was detected in rat testes, along with weaker expression of *Ucn2* and *Ucn3* (Lee et al., 2011). In mammals, CRH and urocortins have important roles in steroidogenesis and fertility (Florio et al., 2004; Murase et al., 2002). In cultured ovarian cells, CRH inhibits steroidogenesis (Calogero et al., 1996), as does Ucn3 (Yata et al., 2009). While the functions of urocortins in teleost gonads remain largely unknown, it is interesting to note that the multitude of these peptides are expressed in both males and females of *A. burtoni*, suggesting a function in reproductive competence could be conserved in vertebrates.

The teleost urohypophysis (caudal neurosecretory system) is located at the caudal end of the spinal cord and regulates homeostasis via neuroendocrine secretion (McCrohan et al., 2007). We found that *A. burtoni* urohypohysis expresses *crhb*, *uts1*, *ucn2*, and *ucn3*. Similarly in zebrafish, *uts1*, *ucn2*, and *ucn3* all showed expression in the caudal spinal cord, where the urohypophysis is located (Parmentier et al., 2008; Parmentier et al., 2011). The rostral region of the spinal cord near the brain in *A. burtoni* also showed expression of *crhb*, *uts1*, *ucn2*, and *ucn3*, although *crhb* and *uts1* expression was only weakly detectable by RT-PCR. In medaka, *uts1*, *ucn2*, and *ucn3* were all found in the spinal cord, but in different spatial localization patterns suggesting different functions (Hosono et al., 2017). Expression of many CRH-family transcripts throughout the spinal cord of fishes, including the urohypophysis, suggest diverse functions including sensory processing, motor output, reproductive function, osmoregulation, ionic homeostasis, and vasopressor activity.

Because our examination of CRH-family genes in peripheral tissues used only end-point RT-PCR, results must be interpreted with caution until additional more sensitive analyses such as in situ hybridization and qPCR are performed. Further understanding of these peptides in *A. burtoni* peripheral tissues will also await more detailed cell-type localization and functional experiments, including receptor distributions and cellular signaling cascades that may differ among CRH-family peptides.

5 | CONCLUSIONS

Here, we provide an extensive description of central and peripheral expression of the urocortins and corticotropin-releasing hormone genes in one species of cichlid fish. Because of the importance of African cichlid species, and *A. burtoni* in particular, as a model for evolution (Brawand et al., 2014), behavior (Fernald & Hirata, 1977), and sensory neuroscience (Maruska & Fernald, 2018), this work will inform future comparative and functional studies. Goals include understanding how the diverse expression patterns have evolved, and how the activity of these peptides regulates adaptive behaviors and physiology. Many genes in *A. burtoni* are regulated during the extensive physiological changes associated with social status and reproductive physiology. Given the importance of CRH and urocortin genes for social interaction and gene expression in mammals, some of the cell populations we identified could play similar roles in fishes.

Identifying the expression patterns, as well as biochemical and physiological functions, of all the CRF family peptides in representatives of distinct vertebrate lineages will be necessary for understanding how this gene family evolved and how the different orthologs play complementary adaptive roles. Further, identifying the expression patterns of CRH receptors, as well as their affinity for CRH and Urocortin peptides, will be necessary to reveal how each of these peptides exerts their effects.

ACKNOWLEDGMENTS

The authors thank members of the Maruska lab for fish maintenance and experimental assistance. Funding was provided by the National Science Foundation (IOS-1456004 and IOS-1456558 to Karen P. Maruska). Julie M. Butler was supported by a Louisiana Board of Regents Fellowship and an NSF Graduate Research Fellowship (1247192).

CONFLICT OF INTEREST

The authors have no known or potential conflicts of interest.

AUTHORS CONTRIBUTION

All authors had full access to the data, take responsibility for the integrity of the data analysis, and approved the final manuscript. Study concept and design: Brian P. Grone, Karen P. Maruska, Julie M. Butler, Christy R. Wayne. Phylogenetic analyses: Brian P. Grone. ISH experiments: Julie M. Butler, Christy R. Wayne, and Karen P. Maruska. RT-PCR and gel electrophoresis: Brian P. Grone and Karen P. Maruska. Analyzed and interpreted the data: Brian P. Grone, Karen P. Maruska, Julie M. Butler, Christy R. Wayne. Manuscript drafts and editing to final form: Brian P. Grone, Karen P. Maruska, Julie M. Butler, Christy R. Wayne. Provided equipment, resources, and funding: Karen P. Maruska.

PEER REVIEW

The peer review history for this article is available at https://publons.com/publon/10.1002/cne.25113.

DATA AVAILABILITY STATEMENT

All of the data used are provided in the manuscript, tables, and figures.

ORCID

Brian P. Grone https://orcid.org/0000-0003-3737-2724
Julie M. Butler https://orcid.org/0000-0002-7400-8780
Karen P. Maruska https://orcid.org/0000-0003-2425-872X

REFERENCES

Aird, F., Clevenger, C. V., Prystowsky, M. B., & Redei, E. (1993). Corticotropin-releasing factor mRNA in rat thymus and spleen. *Proceedings of the National Academy of Sciences of the United States of America*, *90*(15), 7104–7108. https://doi.org/10.1073/pnas.90.15.7104

Alderman, S. L., & Bernier, N. J. (2007). Localization of corticotropin-releasing factor, urotensin I, and CRF-binding protein gene expression in the brain of the zebrafish, *Danio rerio*. *Journal of Comparative Neurology*, *502*(5), 783–793.

Baigent, S. M. (2001). Peripheral corticotropin-releasing hormone and urocortin in the control of the immune response. *Peptides*, *22*(5), 809–820. https://doi.org/10.1016/s0196-9781(01)00395-3

Bale, T. L., & Vale, W. W. (2004). CRF and CRF receptors: Role in stress responsivity and other behaviors. *Annual Review of Pharmacology and Toxicology*, *44*, 525–557. https://doi.org/10.1146/annurev.pharmtox.44.101802.121410

Batten, T. F., Cambre, M. L., Moons, L., & Vandesande, F. (1990). Comparative distribution of neuropeptide-immunoreactive systems in the brain of the green molly, *Poecilia latipinna*. *The Journal of Comparative Neurology*, *302*(4), 893–919. https://doi.org/10.1002/cne.903020416

Biechl, D., Tietje, K., Ryu, S., Grothe, B., Gerlach, G., & Wullimann, M. F. (2017). Identification of accessory olfactory system and medial amygdala in the zebrafish. *Scientific Reports*, *7*, 44295. https://doi.org/10.1038/srep44295

Boorse, G. C., Crespi, E. J., Dautzenberg, F. M., & Denver, R. J. (2005). Urocortins of the south African clawed frog, *Xenopus laevis*: Conservation of structure and function in tetrapod evolution. *Endocrinology*, *146*(11), 4851–4860. https://doi.org/10.1210/en.2005-0497

Brautigam, L., Hillmer, J. M., Soll, I., & Hauptmann, G. (2010). Localized expression of urocortin genes in the developing zebrafish brain. *The Journal of Comparative Neurology*, *518*(15), 2978–2995. https://doi.org/10.1002/cne.22375

Brawand, D., Wagner, C. E., Li, Y. I., Malinsky, M., Keller, I., Fan, S., Simakov, O., Ng, A. Y., Lim, Z. W., Bezault, E., Turner-Maier, J., Johnson, J., Alcazar, R., Noh, H. J., Russell, P., Aken, B., Alföldi, J., Amemiya, C., Azzouzi, N., … di Palma, F. (2014). The genomic substrate for adaptive radiation in African cichlid fish. *Nature*, *513*(7518), 375–381. https://doi.org/10.1038/nature13726

Bu, G., Fan, J., Yang, M., Lv, C., Lin, Y., Li, J., Meng, F., du, X., Zeng, X., Zhang, J., Li, J., & Wang, Y. (2019). Identification of a novel functional Corticotropin-releasing hormone (CRH2) in chickens and its roles in stimulating pituitary TSHbeta expression and ACTH secretion. *Frontiers in Endocrinology*, *10*, 595. https://doi.org/10.3389/fendo.2019.00595

Burmeister, S. S., Munshi, R. G., & Fernald, R. D. (2009). Cytoarchitecture of a cichlid fish telencephalon. *Brain Behav Evol*, *74*(2), 110–120. https://doi.org/10.1159/000235613

Butler, J. M., & Maruska, K. P. (2016). The mechanosensory lateral line system mediates activation of socially-relevant brain regions during territorial interactions. *Frontiers in Behavioral Neuroscience*, *10*, 93. https://doi.org/10.3389/fnbeh.2016.00093

Cabrero, P., Radford, J. C., Broderick, K. E., Costes, L., Veenstra, J. A., Spana, E. P., Davies, S. A., & Dow, J. A. (2002). The Dh gene of *Drosophila melanogaster* encodes a diuretic peptide that acts through cyclic AMP. *The Journal of Experimental Biology*, *205*(Pt 24), 3799–3807.

Calogero, A. E., Burrello, N., Negri-Cesi, P., Papale, L., Palumbo, M. A., Cianci, A., Sanfilippo, S., & D'Agata, R. (1996). Effects of corticotropin-releasing hormone on ovarian estrogen production in vitro. *Endocrinology*, *137*(10), 4161–4166. https://doi.org/10.1210/endo.137.10.8828472

Cardoso, J. C., Bergqvist, C. A., Felix, R. C., & Larhammar, D. (2016). Corticotropin-releasing hormone family evolution: Five ancestral genes remain in some lineages. *Journal of Molecular Endocrinology*, *57*(1), 73–86. https://doi.org/10.1530/JME-16-0051

Cardoso, J. C., Felix, R. C., Bergqvist, C. A., & Larhammar, D. (2014). New insights into the evolution of vertebrate CRH (corticotropin-releasing hormone) and invertebrate DH44 (diuretic hormone 44) receptors in metazoans. *General and Comparative Endocrinology*, *209*, 162–170. https://doi.org/10.1016/j.ygcen.2014.09.004

Carpenter, R. E., Maruska, K. P., Becker, L., & Fernald, R. D. (2014). Social opportunity rapidly regulates expression of CRF and CRF receptors in the brain during social ascent of a teleost fish, *Astatotilapia burtoni*. *PLoS One*, *9*(5), e96632. https://doi.org/10.1371/journal.pone.0096632

Chen, C. C., & Fernald, R. D. (2008). Sequences, expression patterns and regulation of the corticotropin-releasing factor system in a teleost. *General and Comparative Endocrinology*, *157*(2), 148–155. https://doi.org/10.1016/j.ygcen.2008.04.003

Chen, P., Hover, C. V., Lindberg, D., & Li, C. (2012). Central urocortin 3 and type 2 corticotropin-releasing factor receptor in the regulation of energy homeostasis: Critical involvement of the ventromedial hypothalamus. *Front Endocrinol (Lausanne)*, *3*, 180. https://doi.org/10.3389/fendo.2012.00180

Chiu, A. Y., Hunkapiller, M. W., Heller, E., Stuart, D. K., Hood, L. E., & Strumwasser, F. (1979). Purification and primary structure of the neuropeptide egg-laying hormone of *Aplysia californica*. *Proceedings of the National Academy of Sciences of the United States of America*, *76*(12), 6656–6660. https://doi.org/10.1073/pnas.76.12.6656

Coto-Montes, A., Garcia-Fernandez, J. M., del Brio, M. A., & Riera, P. (1994). The distribution of corticotropin-releasing factor immunoreactive neurons and nerve fibres in the brain of Gambusia affinis and *Salmo trutta*. *Histology and Histopathology*, *9*(2), 233–241.

D'Aquila, A. L., Hsieh, A. H., Hsieh, A. H., Almeida, R., Lovejoy, S. R., & Lovejoy, D. A. (2016). Expression and actions of corticotropin-releasing factor/diuretic hormone-like peptide (CDLP) and teneurin C-terminal associated peptide (TCAP) in the vase tunicate, *Ciona intestinalis*: Antagonism of the feeding response. *General and Comparative Endocrinology*, *246*, 105–115. https://doi.org/10.1016/j.ygcen.2016.06.015

Davidson, S. M., Rybka, A. E., & Townsend, P. A. (2009). The powerful cardioprotective effects of urocortin and the corticotropin releasing hormone (CRH) family. *Biochemical Pharmacology*, *77*(2), 141–150. https://doi.org/10.1016/j.bcp.2008.08.033

De Oliveira, A. L., Calcino, A., & Wanninger, A. (2019). Extensive conservation of the proneuropeptide and peptide prohormone complement in mollusks. *Scientific Reports*, *9*(1), 4846. https://doi.org/10.1038/s41598-019-40949-0

Deussing, J. M., & Chen, A. (2018). The Corticotropin-releasing factor family: Physiology of the stress response. *Physiological Reviews*, *98*(4), 2225–2286. https://doi.org/10.1152/physrev.00042.2017

Devetzis, V., Zarogoulidis, P., Kakolyris, S., Vargemezis, V., & Chatzaki, E. (2013). The corticotropin releasing factor system in the kidney: Perspectives for novel therapeutic intervention in nephrology. *Medicinal Research Reviews*, *33*(4), 847–872. https://doi.org/10.1002/med.21268

Dobzhansky, T. (1973). Nothing in biology makes sense except in the light of evolution. *American Biology Teacher*, *35*(3), 125–129.

Endsin, M. J., Michalec, O., Manzon, L. A., Lovejoy, D. A., & Manzon, R. G. (2017). CRH peptide evolution occurred in three phases: Evidence from characterizing sea lamprey CRH system members. *General and Comparative Endocrinology*, *240*, 162–173. https://doi.org/10.1016/j.ygcen.2016.10.009

Fekete, E. M., Inoue, K., Zhao, Y., Rivier, J. E., Vale, W. W., Szücs, A., Koob, G. F., & Zorrilla, E. P. (2007). Delayed satiety-like actions and

altered feeding microstructure by a selective type 2 corticotropin-releasing factor agonist in rats: Intra-hypothalamic urocortin 3 administration reduces food intake by prolonging the post-meal interval. *Neuropsychopharmacology*, *32*(5), 1052–1068. https://doi.org/10.1038/sj.npp.1301214

Fernald, R. D., & Hirata, N. R. (1977). Field study of *Haplochromis burtoni*: Quantitative behavioural observations. *Animal Behaviour*, *25*, 964–975.

Fernald, R. D., & Shelton, L. C. (1985). The organization of the diencephalon and the pretectum in the cichlid fish, Haplochromis burtoni. *J Comp Neurol*, *238*(2), 202–217. https://doi.org/10.1002/cne.902380207

Florio, P., Vale, W., & Petraglia, F. (2004). Urocortins in human reproduction. *Peptides*, *25*(10), 1751–1757. https://doi.org/10.1016/j.peptides.2004.05.026

Fox, H. E., White, S. A., Kao, M. H., & Fernald, R. D. (1997). Stress and dominance in a social fish. *The Journal of Neuroscience*, *17*(16), 6463–6469.

Grommen, S. V. H., Scott, M. K., Darras, V. M., & De Groef, B. (2017). Spatial and temporal expression profiles of urocortin 3 mRNA in the brain of the chicken (*Gallus gallus*). *The Journal of Comparative Neurology*, *525*(11), 2583–2591. https://doi.org/10.1002/cne.24223

Grone, B. P., & Maruska, K. P. (2015a). Divergent evolution of two corticotropin-releasing hormone (CRH) genes in teleost fishes. *Frontiers in Neuroscience*, *9*, 365. https://doi.org/10.3389/fnins.2015.00365

Grone, B. P., & Maruska, K. P. (2015b). A second corticotropin-releasing hormone gene (CRH2) is conserved across vertebrate classes and expressed in the hindbrain of a basal Neopterygian fish, the spotted gar (*Lepisosteus oculatus*). *The Journal of Comparative Neurology*, *523*(7), 1125–1143. https://doi.org/10.1002/cne.23729

Holland, L. Z., & Ocampo Daza, D. (2018). A new look at an old question: When did the second whole genome duplication occur in vertebrate evolution? *Genome Biology*, *19*(1), 209. https://doi.org/10.1186/s13059-018-1592-0

Hosono, K., Kikuchi, Y., Miyanishi, H., Hiraki-Kajiyama, T., Takeuchi, A., Nakasone, K., Maehiro, S., & Okubo, K. (2015). Teleocortin: A novel member of the CRH family in teleost fish. *Endocrinology*, *156*(8), 2949–2957. https://doi.org/10.1210/en.2015-1042

Hosono, K., Yamashita, J., Kikuchi, Y., Hiraki-Kajiyama, T., & Okubo, K. (2017). Three urocortins in medaka: Identification and spatial expression in the central nervous system. *Journal of Neuroendocrinology*, *29*(5), 1–11. https://doi.org/10.1111/jne.12472

Hsu, S. Y., & Hsueh, A. J. (2001). Human stresscopin and stresscopin-related peptide are selective ligands for the type 2 corticotropin-releasing hormone receptor. *Nature Medicine*, *7*(5), 605–611. https://doi.org/10.1038/87936

Huising, M. O., van der Aa, L. M., Metz, J. R., de Fatima Mazon, A., Kemenade, B. M., & Flik, G. (2007). Corticotropin-releasing factor (CRF) and CRF-binding protein expression in and release from the head kidney of common carp: Evolutionary conservation of the adrenal CRF system. *The Journal of Endocrinology*, *193*(3), 349–357. https://doi.org/10.1677/JOE-07-0070

Imaki, J., Imaki, T., Vale, W., & Sawchenko, P. E. (1991). Distribution of corticotropin-releasing factor mRNA and immunoreactivity in the central auditory system of the rat. *Brain Research*, *547*(1), 28–36. https://doi.org/10.1016/0006-8993(91)90571-c

Jain, R., Zwickler, D., Hollander, C. S., Brand, H., Saperstein, A., Hutchinson, B., Brown, C., & Audhya, T. (1991). Corticotropin-releasing factor modulates the immune response to stress in the rat. *Endocrinology*, *128*(3), 1329–1336. https://doi.org/10.1210/endo-128-3-1329

Kageyama, K., Bradbury, M. J., Zhao, L., Blount, A. L., & Vale, W. W. (1999). Urocortin messenger ribonucleic acid: Tissue distribution in the rat and regulation in thymus by lipopolysaccharide and glucocorticoids. *Endocrinology*, *140*(12), 5651–5658. https://doi.org/10.1210/endo.140.12.7223

Kataoka, H., Troetschler, R. G., Li, J. P., Kramer, S. J., Carney, R. L., & Schooley, D. A. (1989). Isolation and identification of a diuretic hormone from the tobacco hornworm, Manduca sexta. *Proceedings of the National Academy of Sciences of the United States of America*, *86*(8), 2976–2980.

Katoh, K., & Standley, D. M. (2013). MAFFT multiple sequence alignment software version 7: Improvements in performance and usability. *Molecular Biology and Evolution*, *30*(4), 772–780. https://doi.org/10.1093/molbev/mst010

Kearse, M., Moir, R., Wilson, A., Stones-Havas, S., Cheung, M., Sturrock, S., Buxton, S., Cooper, A., Markowitz, S., Duran, C., Thierer, T., Ashton, B., Meintjes, P., & Drummond, A. (2012). Geneious basic: An integrated and extendable desktop software platform for the organization and analysis of sequence data. *Bioinformatics*, *28*(12), 1647–1649. https://doi.org/10.1093/bioinformatics/bts199

Kimura, Y., Takahashi, K., Totsune, K., Muramatsu, Y., Kaneko, C., Darnel, A. D., Suzuki, T., Ebina, M., Nukiwa, T., & Sasano, H. (2002). Expression of urocortin and corticotropin-releasing factor receptor subtypes in the human heart. *The Journal of Clinical Endocrinology and Metabolism*, *87*(1), 340–346. https://doi.org/10.1210/jcem.87.1.8160

Kozicz, T., Arimura, A., Maderdrut, J. L., & Lazar, G. (2002). Distribution of urocortin-like immunoreactivity in the central nervous system of the frog *Rana esculenta*. *The Journal of Comparative Neurology*, *453*(2), 185–198. https://doi.org/10.1002/cne.10403

Kozicz, T., Bittencourt, J. C., May, P. J., Reiner, A., Gamlin, P. D., Palkovits, M., Horn, A. K. E., Toledo, C. A. B., & Ryabinin, A. E. (2011). The Edinger-Westphal nucleus: A historical, structural, and functional perspective on a dichotomous terminology. *The Journal of Comparative Neurology*, *519*(8), 1413–1434. https://doi.org/10.1002/cne.22580

Kozicz, T., Yanaihara, H., & Arimura, A. (1998). Distribution of urocortin-like immunoreactivity in the central nervous system of the rat. *The Journal of Comparative Neurology*, *391*(1), 1–10.

Lederis, K., Letter, A., McMaster, D., Moore, G., & Schlesinger, D. (1982). Complete amino acid sequence of urotensin I, a hypotensive and corticotropin-releasing neuropeptide from Catostomus. *Science*, *218*(4568), 162–165.

Lee, S., Braden, B., Kang, S. S., & Rivier, C. (2011). Urocortins are present in the rat testis. *Neuropeptides*, *45*(2), 131–137. https://doi.org/10.1016/j.npep.2010.12.006

Lewis, K., Li, C., Perrin, M. H., Blount, A., Kunitake, K., Donaldson, C., Vaughan, J., Reyes, T. M., Gulyas, J., Fischer, W., Bilezikjian, L., Rivier, J., Sawchenko, P. E., & Vale, W. W. (2001). Identification of urocortin III, an additional member of the corticotropin-releasing factor (CRF) family with high affinity for the CRF2 receptor. *Proceedings of the National Academy of Sciences USA*, *98*(13), 7570–7575. https://doi.org/10.1073/pnas.121165198

Lim, M. M., Tsivkovskaia, N. O., Bai, Y., Young, L. J., & Ryabinin, A. E. (2006). Distribution of corticotropin-releasing factor and urocortin 1 in the vole brain. *Brain, Behavior and Evolution*, *68*(4), 229–240. https://doi.org/10.1159/000094360

Lovejoy, D. A., & Barsyte-Lovejoy, D. (2010). Characterization of a corticotropin-releasing factor (CRF)/diuretic hormone-like peptide from tunicates: Insight into the origins of the vertebrate CRF family. *General and Comparative Endocrinology*, *165*(2), 330–336. https://doi.org/10.1016/j.ygcen.2009.07.013

Lovejoy, D. A., Chang, B. S., Lovejoy, N. R., & del Castillo, J. (2014). Molecular evolution of GPCRs: CRH/CRH receptors. *Journal of Molecular Endocrinology*, *52*(3), T43–T60. https://doi.org/10.1530/JME-13-0238

Lovejoy, D. A., & de Lannoy, L. (2013). Evolution and phylogeny of the corticotropin-releasing factor (CRF) family of peptides: Expansion and specialization in the vertebrates. *Journal of Chemical Neuroanatomy.*, *54*, 50–56. https://doi.org/10.1016/j.jchemneu.2013.09.006

Mancera, J. M., & Fernández-Llebrez, P. (1995). Localization of Corticotropin-releasing factor immunoreactivity in the brain of the teleost Sparus-Aurata. *Cell and Tissue Research*, *281*(3), 569–572.

Maruska, K. P., & Fernald, R. D. (2010). Behavioral and physiological plasticity: Rapid changes during social ascent in an African cichlid fish. *Hormones and Behavior*, *58*(2), 230–240. https://doi.org/10.1016/j.yhbeh.2010.03.011

Maruska, K. P., Butler, J. M., Field, K. E., & Porter, D. T. (2017). Localization of glutamatergic, GABAergic, and cholinergic neurons in the brain of the African cichlid fish, Astatotilapia burtoni. *J Comp Neurol*, *525*(3), 610–638. https://doi.org/10.1002/cne.24092

Maruska, K. P., & Fernald, R. D. (2018). *Astatotilapia burtoni*: A model system for analyzing the neurobiology of behavior. *ACS Chemical Neuroscience*, *9*(8), 1951–1962. https://doi.org/10.1021/acschemneuro.7b00496

Matz, S. P., & Hofeldt, G. T. (1999). Immunohistochemical localization of corticotropin-releasing factor in the brain and corticotropin-releasing factor and thyrotropin-stimulating hormone in the pituitary of chinook salmon (*Oncorhynchus tshawytscha*). *General and Comparative Endocrinology*, *114*(1), 151–160. https://doi.org/10.1006/gcen.1999.7253

McCrohan, C. R., Lu, W., Brierley, M. J., Dow, L., & Balment, R. J. (2007). Fish caudal neurosecretory system: A model for the study of neuroendocrine secretion. *General and Comparative Endocrinology*, *153*(1–3), 243–250. https://doi.org/10.1016/j.ygcen.2006.12.027

Miller, M. A., Pfeiffer, W., and Schwartz, T. (2010). *Creating the CIPRES Science Gateway for inference of large phylogenetic trees*. Paper presented at the Proceedings of the Gateway Computing Environments Workshop (GCE).

Morin, S. M., Ling, N., Liu, X. J., Kahl, S. D., & Gehlert, D. R. (1999). Differential distribution of urocortin- and corticotropin-releasing factor-like immunoreactivities in the rat brain. *Neuroscience*, *92*(1), 281–291. https://doi.org/10.1016/s0306-4522(98)00732-5

Mueller, T., Vernier, P., & Wullimann, M. F. (2004). The adult central nervous cholinergic system of a neurogenetic model animal, the zebrafish *Danio rerio*. *Brain Research*, *1011*(2), 156–169. https://doi.org/10.1016/j.brainres.2004.02.073

Muñoz-Cueto, J., Sarasquete, C., Zohar, Y., & Kah, O. (2001). *An atlas of the brain of the gilthead seabream (Sparus aurata)*. College Park, Md.: Maryland Sea Grant.

Murase, M., Uemura, T., Kondoh, Y., Funabashi, T., & Hirahara, F. (2002). Role of corticotropin-releasing hormone in ovarian steroidogenesis. *Endocrine*, *18*(3), 255–260. https://doi.org/10.1385/ENDO:18:3:255

Nazarloo, H. P., Buttrick, P. M., Saadat, H., & Dunn, A. J. (2006). The roles of corticotropin-releasing factor-related peptides and their receptors in the cardiovascular system. *Current Protein & Peptide Science*, *7*(3), 229–239. https://doi.org/10.2174/138920306777452358

Nock, T. G., Chand, D., & Lovejoy, D. A. (2011). Identification of members of the gonadotropin-releasing hormone (GnRH), corticotropin-releasing factor (CRF) families in the genome of the holocephalan, *Callorhinchus milii* (elephant shark). *General and Comparative Endocrinology*, *171*(2), 237–244. https://doi.org/10.1016/j.ygcen.2011.02.001

Parmentier, C., Hameury, E., Dubessy, C., Quan, F. B., Habert, D., Calas, A., Vaudry, H., Lihrmann, I., & Tostivint, H. (2011). Occurrence of two distinct urotensin II-related peptides in zebrafish provides new insight into the evolutionary history of the urotensin II gene family. *Endocrinology*, *152*(6), 2330–2341. https://doi.org/10.1210/en.2010-1500

Parmentier, C., Hameury, E., Lihrmann, I., Taxi, J., Hardin-Pouzet, H., Vaudry, H., Calas, A., & Tostivint, H. (2008). Comparative distribution of the mRNAs encoding urotensin I and urotensin II in zebrafish. *Peptides*, *29*(5), 820–829. https://doi.org/10.1016/j.peptides.2008.01.023

Pepels, P. P., Meek, J., Wendelaar Bonga, S. E., & Balm, P. H. (2002). Distribution and quantification of corticotropin-releasing hormone (CRH) in the brain of the teleost fish *Oreochromis mossambicus* (tilapia). *The Journal of Comparative Neurology*, *453*(3), 247–268. https://doi.org/10.1002/cne.10377

Porter, D. T., Roberts, D. A., & Maruska, K. P. (2017). Distribution and female reproductive state differences in orexigenic and anorexigenic neurons in the brain of the mouth brooding African cichlid fish, *Astatotilapia burtoni*. *The Journal of Comparative Neurology*, *525*(14), 3126–3157. https://doi.org/10.1002/cne.24268

Potter, E., Behan, D. P., Linton, E. A., Lowry, P. J., Sawchenko, P. E., & Vale, W. W. (1992). The central distribution of a corticotropin-releasing factor (CRF)-binding protein predicts multiple sites and modes of interaction with CRF. *Proceedings of the National Academy of Sciences of the United States of America*, *89*(9), 4192–4196. https://doi.org/10.1073/pnas.89.9.4192

Prater, C. M., Garcia, C., McGuire, L. P., & Carr, J. A. (2018). Tectal corticotropin-releasing factor (CRF) neurons respond to fasting and a reactive stressor in the African Clawed Frog, *Xenopus laevis*. *General and Comparative Endocrinology*, *258*, 91–98. https://doi.org/10.1016/j.ygcen.2017.07.029

Rambaut, A., Drummond, A. J., Xie, D., Baele, G., & Suchard, M. A. (2018). Posterior summarization in Bayesian Phylogenetics Using Tracer 1.7. *Systematic Biology*, *67*(5), 901–904. https://doi.org/10.1093/sysbio/syy032

Reyes, T. M., Lewis, K., Perrin, M. H., Kunitake, K. S., Vaughan, J., Arias, C. A., Hogenesch, J. B., Gulyas, J., Rivier, J., Vale, W. W., & Sawchenko, P. E. (2001). Urocortin II: A member of the corticotropin-releasing factor (CRF) neuropeptide family that is selectively bound by type 2 CRF receptors. *Proceedings of the National Academy of Sciences*, *98*(5), 2843–2848. https://doi.org/10.1073/pnas.051626398

Risbrough, V. B., Hauger, R. L., Pelleymounter, M. A., & Geyer, M. A. (2003). Role of corticotropin releasing factor (CRF) receptors 1 and 2 in CRF-potentiated acoustic startle in mice. *Psychopharmacology*, *170*(2), 178–187. https://doi.org/10.1007/s00213-003-1535-6

Rivier, C., & Vale, W. (1984). Influence of corticotropin-releasing factor on reproductive functions in the rat. *Endocrinology*, *114*(3), 914–921. https://doi.org/10.1210/endo-114-3-914

Ronquist, F., Teslenko, M., van der Mark, P., Ayres, D. L., Darling, A., Hohna, S., Larget, B., Liu, L., Suchard, M. A., & Huelsenbeck, J. P. (2012). MrBayes 3.2: Efficient Bayesian phylogenetic inference and model choice across a large model space. *Systematic Biology*, *61*(3), 539–542. https://doi.org/10.1093/sysbio/sys029

Slominski, A., Roloff, B., Curry, J., Dahiya, M., Szczesniewski, A., & Wortsman, J. (2000). The skin produces urocortin. *The Journal of Clinical Endocrinology and Metabolism*, *85*(2), 815–823. https://doi.org/10.1210/jcem.85.2.6381

Slominski, A. T., Zmijewski, M. A., Zbytek, B., Tobin, D. J., Theoharides, T. C., & Rivier, J. (2013). Key role of CRF in the skin stress response system. *Endocrine Reviews*, *34*(6), 827–884. https://doi.org/10.1210/er.2012-1092

Spina, M., Merlo-Pich, E., Chan, R. K., Basso, A. M., Rivier, J., Vale, W., & Koob, G. F. (1996). Appetite-suppressing effects of urocortin, a CRF-related neuropeptide. *Science*, *273*(5281), 1561–1564.

Stenzel-Poore, M. P., Heldwein, K. A., Stenzel, P., Lee, S., & Vale, W. W. (1992). Characterization of the genomic corticotropin-releasing factor (CRF) gene from *Xenopus laevis*: Two members of the CRF family exist in amphibians. *Molecular Endocrinology*, *6*(10), 1716–1724. https://doi.org/10.1210/mend.6.10.1448118

Takahashi, K., Totsune, K., Murakami, O., Saruta, M., Nakabayashi, M., Suzuki, T., Sasano, H., & Shibahara, S. (2004). Expression of urocortin III/stresscopin in human heart and kidney. *The Journal of Clinical Endocrinology & Metabolism*, *89*(4), 1897–1903. https://doi.org/10.1210/jc.2003-031663

Takahashi, K., Totsune, K., Sone, M., Murakami, O., Satoh, F., Arihara, Z., Sasano, H., Iino, K., & Mouri, T. (1998). Regional distribution of urocortin-like immunoreactivity and expression of urocortin mRNA in the human brain. *Peptides*, *19*(4), 643–647. https://doi.org/10.1016/s0196-9781(98)00012-6

Tang, N., Zhang, X., Wang, S., Qi, J., Tian, Z., Wang, B., Chen, H., Wu, Y., Wang, M., Xu, S., Chen, D., & Li, Z. (2019). UCN3 suppresses food intake in coordination with CCK and the CCK2R in Siberian sturgeon

(*Acipenser baerii*). *Comparative Biochemistry and Physiology Part A: Molecular & Integrative Physiology*, *234*, 106–113. https://doi.org/10.1016/j.cbpa.2019.04.022

Vale, W., Spiess, J., Rivier, C., & Rivier, J. (1981). Characterization of a 41-residue ovine hypothalamic peptide that stimulates secretion of corticotropin and beta-endorphin. *Science*, *213*(4514), 1394–1397.

Vandenborne, K., De Groef, B., Geelissen, S. M., Boorse, G. C., Denver, R. J., Kuhn, E. R., Darras, V. M., & Van der Geyten S. (2005). Molecular cloning and developmental expression of corticotropin-releasing factor in the chicken. *Endocrinology*, *146*(1), 301–308. https://doi.org/10.1210/en.2004-0608

Vaughan, J., Donaldson, C., Bittencourt, J., Perrin, M. H., Lewis, K., Sutton, S., Chan, R., Turnbull, A. V., Lovejoy, D., Rivier, C., Rivier, J., Sawchenko, P. E., & Vale, W. (1995). Urocortin, a mammalian neuropeptide related to fish urotensin I and to corticotropin-releasing factor. *Nature*, *378*(6554), 287–292. https://doi.org/10.1038/378287a0

Wagle, M., Mathur, P., & Guo, S. (2011). Corticotropin-releasing factor critical for zebrafish camouflage behavior is regulated by light and sensitive to ethanol. *The Journal of Neuroscience*, *31*(1), 214–224. https://doi.org/10.1523/JNEUROSCI.3339-10.2011

Wang, T., Zhou, C., Yuan, D., Lin, F., Chen, H., Wu, H., Wei, R., Xin, Z., Liu, J., Gao, Y., & Li, Z. (2014). *Schizothorax prenanti* corticotropin-releasing hormone (CRH): Molecular cloning, tissue expression, and the function of feeding regulation. *Fish Physiol Biochem*, *40*(5), 1407–1415. https://doi.org/10.1007/s10695-014-9935-6

Williams, T. A., Bergstrome, J. C., Scott, J., & Bernier, N. J. (2017). CRF and urocortin 3 protect the heart from hypoxia/reoxygenation-induced apoptosis in zebrafish. *American Journal of Physiology. Regulatory, Integrative and Comparative Physiology*, *313*(2), R91–R100. https://doi.org/10.1152/ajpregu.00045.2017

Wullimann, M. F., Rupp, B., & Reichert, H. (1996). *Neuroanatomy of the zebrafish brain: a topological atlas*. Basel, Switzerland: Birkhauser Verlag.

Yata, A., Nakabayashi, K., Wakahashi, S., Maruo, N., Ohara, N., & Maruo, T. (2009). Suppression of progesterone production by stresscopin/urocortin 3 in cultured human granulosa-lutein cells. *Human Reproduction*, *24*(7), 1748–1753. https://doi.org/10.1093/humrep/dep063

Ye, C., Xu, S. H., Hu, Q. Y., Zhou, L. L., Qin, X. F., Jia, J. Y., & Hu, G. F. (2019). Global view of neuropeptides and their receptors in the brain and pituitary of grass carp (Ctenopharyngodon idellus). *Aquaculture*, *512*, 734360. https://doi.org/10.1016/j.aquaculture.2019.734360

Yulis, C. R., Lederis, K., Wong, K. L., & Fisher, A. W. (1986). Localization of urotensin I- and corticotropin-releasing factor-like immunoreactivity in the central nervous system of *Catostomus commersoni*. *Peptides*, *7*(1), 79–86. https://doi.org/10.1016/0196-9781(86)90065-3

Zupanc, G. K., Horschke, I., & Lovejoy, D. A. (1999). Corticotropin releasing factor in the brain of the gymnotiform fish, *Apteronotus leptorhynchus*: Immunohistochemical studies combined with neuronal tract tracing. *General and Comparative Endocrinology*, *114*(3), 349–364. https://doi.org/10.1006/gcen.1999.7273

How to cite this article: Grone BP, Butler JM, Wayne CR, Maruska KP. Expression patterns and evolution of urocortin and corticotropin-releasing hormone genes in a cichlid fish. *J Comp Neurol*. 2021;529:2596–2619. https://doi.org/10.1002/cne.25113